



## Design, formulation and *in-vitro* characterization of Irbesartan solid self-nanoemulsifying drug delivery system (S-SNEDDS) prepared using spray drying technique

Ali M. Nasr<sup>1\*</sup>, Ahmed R. Gardouh<sup>2</sup>, Hassan M. Ghonaim<sup>2</sup> and Mamdouh M. Ghorab<sup>2</sup>

<sup>1</sup>Department of Pharmaceutics, Faculty of Pharmacy and Pharmaceutical Industry, Sinai University, Alarish, Egypt

<sup>2</sup>Department of Pharmaceutics, Faculty of Pharmacy, Suez Canal University, Ismailia, Egypt

### ABSTRACT

The main objective of this study was to develop solid self-nanoemulsifying drug delivery system (S-SNEDDS) of Irbesartan (IRB) for enhancement of its solubility and dissolution rate. In this study, a novel liquid SNEDDS containing Irbesartan was formulated and further developed into a solid form by spray drying technique using Aerosil 200 as solid carrier. The solubility of IRB was determined in various oils, surfactants and co-surfactants to select the best candidates for IRB for further study. Pseudoternary phase diagrams were constructed to identify the efficient area of self-nanoemulsification. Based on preliminary screening of different unloaded SNEDDS formulae, eight formulae of IRB loaded SNEDDS were prepared using Capryol 90, Cremophor RH40 and Transcutol HP as oil, surfactant and cosurfactant respectively. The optimized IRB loaded SNEDDS formulae were evaluated for effect of dilution (with different volumes at different pH values), efficiency of self-emulsification, viscosity, optical clarity, morphological characterization, drug loading efficiency, *in-vitro* drug release, droplet size analysis as well as polydispersity index (PDI). SNEDDS formulae were also tested for thermodynamic stability and zeta potential to confirm the stability of the prepared SNEDDS. Results showed that the mean droplet size of all reconstituted SNEDDS was found to be in the nanometric range with optimum PDI values. All formulae also showed rapid emulsification time, good optical clarity, and high drug content; and found to be highly stable. Transmission electron microscopic images showed the formation of spherical and homogeneous droplets with a size smaller than 50nm, which satisfies the criteria of nanometric size range required for nanoemulsifying formulae. *In-vitro* release of IRB from SNEDDS formulae showed that more than 99% of IRB release in approximately 90 minutes. Optimized SNEDDS formulae with the smallest particle size, rapid emulsification time, best optical clarity, and maximum drug content and rapid *in-vitro* release were selected to be developed into solid self-nanoemulsifying drug delivery system (S-SNEDDS) using spray drying technique. The prepared S-SNEDDS formulae were evaluated for flow properties, differential scanning calorimetry (DSC), scanning electron microscopy (SEM), reconstitution properties, drug content and *in-vitro* dissolution study. It was found that S-SNEDDS formulae showed good flow properties and high drug content. Reconstitution properties of S-SNEDDS showed spontaneous self-nanoemulsification and no sign of phase separation. DSC thermograms revealed that IRB was in solubilized form and FTIR supported these findings. SEM photographs showed smooth uniform surface of S-SNEDDS with less aggregation. Results of the *in-vitro* drug release showed that there was great enhancement in dissolution rate of IRB.

**Keywords:** Solid Self-nanoemulsifying drug delivery system (S-SNEDDS), Irbesartan, Spray drying, Aerosil 200, Capryol 90, Cremophor RH40 and Transcutol HP.

### INTRODUCTION

The improvement of bioavailability of drugs represents one of the greatest challenges in drug formulations. Most of new drug candidates reveal poor water solubility which leads to poor oral bioavailability, high intra- and inter-

subject variability and lack of dose proportionality [1]. One of the most popular and commercially viable formulation strategies for this challenge is self-nanoemulsifying drug delivery systems (SNEDDS) [2]. Basically, SNEDDS are isotropic and thermodynamically stable mixtures of oil, surfactant, cosurfactant and drug that form fine oil-in-water (o/w) nanoemulsion when added to aqueous phases under gentle agitation [3]. Upon administration, the isotropic mixture will come in contact with the aqueous phase of gastrointestinal tract and form an oil-in-water nanoemulsion with the aid of gastrointestinal motility. This spontaneous formation of nanoemulsion in the gastrointestinal tract presents the drug in solubilized form inside small droplets of oil, all over its transit through the GIT [4]. The nano-sized droplets provide also a large interfacial surface area for drug release and absorption. Conventional SNEDDS are usually prepared as liquid dosage forms that can be administered in soft gelatin capsules [5], which have some limitations such as: high production cost, incompatibility problems with capsule shell [6], low drug portability and stability, drug leakage and precipitation, low drug loading, few choices of dosage forms and irreversible drugs/excipients precipitation. More importantly the large quantity of surfactants in the formulations can induce gastrointestinal irritations [7].

In recent years, much attention has been paid to solid self-nanoemulsifying drug delivery systems (S-SNEDDS), which have shown lots of reasonable successes in improving oral bioavailability of poorly soluble drugs [8]. This novel drug delivery system combines the advantages of liquid SNEDDS with those of a solid dosage form and overcomes the limitations associated with liquid formulations [9]. S-SNEDDS exhibited also more commercial potential and patient acceptability [10]. Many techniques are offered to convert conventional liquid SNEDDS to solid form such as spray drying, adsorptions to solid carriers, spray cooling, melt extrusion, melt granulation, supercritical fluid based methods and high pressure homogenization. The resulting powder may then be filled directly into hard gelatin capsules or mixed with suitable excipients before compression into tablets.

Irbesartan is novel selective angiotensin II receptor blocker that is approved for the treatment of hypertension [11]. Irbesartan is slightly soluble in alcohol and methylene chloride and practically insoluble in water (0.00884 mg/ml) due to its hydrophobic nature as shown in figure (1). Irbesartan is currently marketed as tablet (75, 150 and 300mg) presently available conventional formulation. The estimated bioavailability of IRB is greater than 60%; however plasma level do not increase proportionally with dose. The calculated biopharmaceutical parameter suggests that IRB has very low absorbable dose. Also volume of aqueous medium required to dissolve highest dose, calculated using ratio of dose/solubility was 20L. Thus, theoretically IRB exhibits a solubility limited bioavailability and would be advantageous to enhance solubility and dissolution rate of IRB [12]. To overcome this problem there was a need to develop S-SNEDDS which improves the oral bioavailability of Irbesartan. Hence the present study aimed towards development of a novel S-SNEDDS of IRB by spray drying technique using Aerosil 200 as solid carrier for enhanced bioavailability.

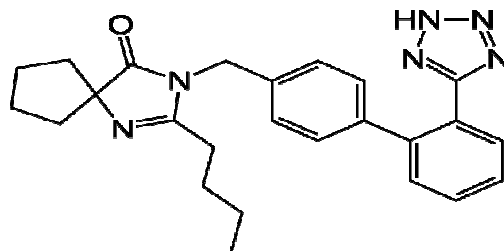


**Fig. 1. Chemical Structure of Irbesartan**

## EXPERIMENTAL SECTION

### 2.1. Materials

Irbesartan(2-butyl-3-({4-[2-(2*H*-1,2,3,4-tetrazol-5-yl)phenyl] phenyl)methyl)-1,3diazaspiro [4.4]non-1-en-4-one), Miglyol 812 (Caprylic/Capric Triglyceride), Miglyol 818 (Caprylic/ Capric/Linoleic Triglyceride), Miglyol 829 (Caprylic/Capric/Succinic Triglyceride), Labrafil M 1944 CS (Oleoyl polyoxyl-6 glycerides) and Aerosil 200 (Silicon Dioxide) (gift from Medical Union Pharmaceuticals, Egypt), Capryol 90 (Propylene glycol monocaprylate), Gelucire 44/14 (Lauroyl polyoxyl-32 glycerides), Lauroglycol FCC (Propylene glycol laurate), Labrafac lipophile WL 1349 (Caprylic/Capric Triglyceride), Maisine 35-1 (Glyceryl Linoleate) and Transcutol HP (2-(2-Ethoxyethoxy)ethanol) (Gattefossé, France), Cremophor RH40, Cremophor S9 and Labrasol (Nerol Chemicals, Egypt), Bitter almond oil, Castor oil, Olive oil, Cotton seed oil, Arachis oil, Oleic acid, Hydrochloric acid and Propylene Glycol (El Nasr Pharmaceutical Chemicals, Egypt), Tween 20, Tween 40, Tween 60, Tween 80, Span 20, Span 80, PEG 400, PEG 600 and Sodium Hydroxide (Oxford Laboratory, India), PEG 200 (Loba Chem. Pvt. Ltd.,

India), Glycerin (El Gomhouria Pharmaceuticals, Egypt) and Sodium Dihydrogen Phosphate (PureLab, USA). Other chemicals are of HPLC grade

## 2.2. Methods

### 2.2.1. Preformulation Study (Selection of SNEDDS Components)

#### 2.2.1.1. Study of IRB solubility in various oils, surfactants and cosurfactants

Selection of SNEDDS components was based upon the maximum solubility of IRB in various oils, surfactants and cosurfactants. Different oils including Gelucire 44/14, Lauroglycol FCC, Labrafac lipophile WL 1349, Capryol 90, Labrafil M 1944 CS, Miglyol 812, Miglyol 818, Miglyol 829, Maisine 35-1, Bitter almond oil, Castor oil, Olive oil, Cotton seed oil, Arachis oil and Oleic acid were taken for the study. Also various surfactants (Cremophor RH40, Cremophor S9, Labrasol, Tween 20, Tween 40, Tween 60, Tween 80, Span 20 and Span 80) and cosurfactants including Transcutol HP, PEG 200, PEG 400, PEG 600, Propylene glycol and Glycerin were also screened. In this study, an excess amount of IRB (approximately 500 mg) was introduced into 2mL of each vehicle in screw capped greiner tubes. The mixtures were mixed well using a vortex mixer (Maximix II, USA) for 10 minutes to enhance the proper mixing of IRB with the vehicles and thus facilitate the solubilization. The obtained mixtures were then shaken for 72 hours in an isothermal mechanical shaker (Clifton shaking water bath, UK) maintained at 40°C to attain equilibrium. After reaching equilibrium, the equilibrated samples were centrifuged at 3000 r.p.m for 15 minutes to precipitate the undissolved IRB. Aliquots from the supernatants were then withdrawn and filtered through a membrane filter (0.45µm, Whatmann). Filtered solutions were suitably diluted with methanol and IRB concentrations were determined using Hitachi UV-Vis spectrophotometer (Hitachi U-2900, Japan) at  $\lambda_{\text{max}}$  246nm. All measurements were done in triplicate and the solubility was expressed as the mean value (mg/mL)  $\pm$  SD [13].

#### 2.2.1.2. Preliminary screening of surfactants for emulsification efficiency

Different surfactants (Cremophor RH40, Cremophor S 9, Labrasol, Tween 20, Tween 40, Tween 60, Tween 80, Span 20 and Span 80) were screened for its emulsification ability in the selected oily phase. Surfactant selection was done on the basis of transparency percentage and ease of emulsification [14]. Briefly, 500µL of each surfactant was added to 500µL of the selected oil. The mixtures were gently heated at 50°C for 2 minutes to attain homogenization of components. From each mixture, 100µL were then diluted with distilled water up to 50mL in glass stoppered flask. The stoppered flasks were inverted several times and the number of flask inversions required to form a homogenous nanoemulsion (with no turbidity or phase separation) was counted. Furthermore, the formed emulsions were allowed to stand for 2 hours and their percentage of transmittance was assessed at 650 nm (by means of UV-Vis Spectrophotometer) using distilled water as blank. The percentage of transmittance was calculated for each emulsion in triplicates and the average values  $\pm$  SD were calculated. The surfactant forming a clear emulsion with fewer inversions and higher percentage of transmittance was selected [15].

#### 2.2.1.3. Preliminary screening of cosurfactants for emulsification efficiency

The selected oily phase and surfactant were used for further screening of the different co-surfactants (Transcutol HP, PEG 200, PEG 400, PEG 600, Propylene glycol and Glycerin) for their emulsification efficiency. Mixtures of 200µL of co-surfactant, 400µL of selected surfactant and 600µL of selected oil were prepared and evaluated in the same manner as described in preliminary screening of surfactants [16].

#### 2.2.1.4. Construction of pseudoternary phase diagram

In order to investigate concentration range of components for the existing boundary of SNEDDS, pseudoternary phase diagrams were constructed using the water titration method at room temperature [17]. The ratio of surfactant to cosurfactant ( $S_{\text{mix}}$ ) was also optimized using pseudoternary phase diagrams. The selected oil, surfactant and cosurfactant were grouped in different combinations for phase studies. Surfactant and co-surfactant ( $S_{\text{mix}}$ ) in each group were mixed in different weight ratio (1:0, 1:1, 1:2, 1:3, 2:1 and 3:1). These  $S_{\text{mix}}$  ratios were chosen in increasing concentration of surfactant with respect to cosurfactant and in increasing concentration of cosurfactant with respect to surfactant. For each phase diagram, oil and specific  $S_{\text{mix}}$  ratio are mixed thoroughly in different weight ratios (1:9, 1:7, 1:5, 1:4, 1:3, 1:2, 1:1 and 2:1) in different glass vials. Different ratios of oils and  $S_{\text{mix}}$  were made to delineate the boundaries of phase precisely [18]. The amount of aqueous phase was incremented by 5% to provide concentration of aqueous phase in the range of 5–95% of total volumes. After each addition of aqueous phase, the mixtures in the vials were vortexed for 2 minutes and allowed to equilibrate. The change in physical states from transparent to turbid and vice-versa were visually observed and marked on the three component ternary phase diagram where each axis represented the oil,  $S_{\text{mix}}$  and water, respectively. The different phase diagrams were plotted using CHEMIX ternary plot software (CHEMIX School Ver. 3.60, Pub. Arne Standnes).

### 2.2.2. Preparation of IRB loaded SNEDDS

Once the nanoemulsifying region was identified, SNEDDS formulae with desired component ratios were selected for IRB incorporation and further optimization. A series of SNEDDS formulae were prepared with varying weight

ratios of selected oil (5–15% w/w) and Smix (20–80% w/w) as presented in table (1). In all formulae, the amount of IRB was kept constant. Briefly oil, surfactant and cosurfactant were accurately weighed and mixed in stoppered glass vials using a vortex mixer to ensure complete mixing. Amount of IRB was dispersed into the mixture of oil and Smix with continuous mixing until IRB was completely dissolved. These systems were warmed to 40°C using a water bath for 30 minutes with mild shaking until a clear solution was obtained. The prepared formulae were then stored at room temperature until further use [19].

Tab. 1. Percent w/w compositions of optimized IRB loaded SNEDDS formulae

| Formula | IRB (mg) | Oil (% w/w) | Smix (% w/w) |
|---------|----------|-------------|--------------|
| F1      | 75       | 5           | 20           |
| F2      | 75       | 5           | 40           |
| F3      | 75       | 5           | 60           |
| F4      | 75       | 5           | 80           |
| F5      | 75       | 8.5         | 60           |
| F6      | 75       | 8.5         | 80           |
| F7      | 75       | 11.5        | 60           |
| F8      | 75       | 11.5        | 80           |

### 2.2.3. Characterization and Evaluation of IRB loaded SNEDDS

#### 2.2.3.1. Thermodynamic stability studies

The prepared SNEDDS formulae were subjected to heating-cooling cycles, centrifugation and freeze-thaw cycles, where the physical appearances of the formulae were visually observed at the end of each testing. In heating cooling cycles, the prepared formulae were subjected to six cycles between refrigerator temperature 4°C and 45°C with storage at each temperature for 48 hours. The formulae that did not show any phase separations, creaming or cracking were subjected to centrifugation at 3500 rpm for 30 minutes. Finally, only formulae which passed the previous two steps were stored at alternating temperatures of -21°C and 25°C, with the duration of 48 hours at each temperature, for three cycles [20].

#### 2.2.3.2. Robustness to dilution

In order to simulate *in-vivo* dilution behavior, effect of dilution on emulsion characteristics was studied. Robustness of different SNEDDS formulae to dilution was done by diluting 1 mL of each formula 10, 100 and 1000 times with distilled water, 0.1 N HCl and phosphate buffer of pH 6.8. The diluted systems were mixed using a magnetic stirrer at 37°C to simulate body temperature and gastric motility in the gastrointestinal tract till complete homogeneity. These systems were stored at ambient temperature for 24 hours then visually observed for any signs of phase separation [21].

#### 2.2.3.3. Assessment of efficiency of self-emulsification

The self-emulsification efficiency of SNEDDS was evaluated using a standard USP dissolution apparatus type II (Erweka, DT 600, Germany). 1 mL of each formula was added to 500 mL of distilled water maintained at 37±0.5°C. Gentle agitation was provided by a standard stainless steel dissolution paddle rotating at 50 rpm. The prepared formulae were assessed visually according to the rate of emulsification and final appearance of the nanoemulsion. The *in-vitro* performance of the formulation was visually evaluated using the following grading system [22].

Grade A: Rapidly forming emulsion having a clear or bluish appearance (within 1 minute).

Grade B: Rapidly forming, slightly less clear emulsion, having a bluish white appearance.

Grade C: Fine milky emulsion that formed within 2 minutes.

Grade D: Dull, grayish white emulsion having slightly oily appearance that is slow to emulsify (longer than 2 minutes).

Grade E: Formula exhibiting either poor or minimal emulsification with large oil globules present on the surface.

#### 2.2.3.4. Self-emulsification time

In this test, a predetermined volume of each formula (1 mL) was introduced into 300 mL of distilled water maintained at 37±0.5°C in a glass beaker and the contents mixed gently using a magnetic stirrer rotating at constant speed. The emulsification time (the time required for a pre-concentrate to form a homogeneous mixture upon dilution) was monitored by visually observing the disappearance of SNEDDS and the final appearance of the nanoemulsion [23].

#### 2.2.3.5. Viscosity determination

The viscosity of the prepared SNEDDS formulae was measured at 25±0.5°C as such before and after dilution by Brookfield viscometer (Brookfield Engineering Labs, USA) using spindle CC3-14 with shear rate at 100 rpm [24].

#### **2.2.3.6. Spectroscopic characterization of optical clarity**

The optical clarity of aqueous dispersions of SNEDDS formulae was measured spectrophotometrically. Composition was prepared according to the design and diluted to 100 times with distilled water. The percentage transmittance as measurements of optical clarity for the prepared SNEDDS formulae was measured at 650 nm using distilled water as the standard blank solution [25].

#### **2.2.3.7. Transmission electron microscopy (TEM)**

The surface morphology and globule size of the prepared SNEDDS formulae were observed using Transmission electron microscopy (JEM-2100, USA). Prior to analysis, the SNEDDS samples were diluted 10 times with distilled water. A drop from the resultant nanoemulsion was deposited on a film-coated copper grid forming a thin liquid film. The films were then negatively stained with 2% (w/v) phosphotungstic acid solution. After air drying, the stained films were photographed by transmission electron microscopy [26].

#### **2.2.3.8. Droplet size analysis and polydispersibility Index (PDI) determination**

The droplet size is an important factor in self-emulsification performance because it determines the rate and extent of drug release as well as absorption. Prior to measurement, 1mL of each SNEDDS formula was diluted 10 times with distilled water. The globule size and polydispersibility index of the formed nanoemulsions were determined by dynamic light scattering (DLS) using a photon correlation spectrometer (Zetasizer, Malvern Instruments LTD, UK) which analyzes the fluctuations in light scattering due to Brownian motion of the particles. Light scattering was monitored at 25°C at scattering angle 90° [27].

#### **2.2.3.9. Zeta potential determination**

The zeta potential of the diluted SNEDDS formulae was determined using Zetasizer (Malvern Instruments, UK). Samples were placed in clear disposable zeta cells and results were recorded. Charge on emulsion droplets and their zeta potential values were obtained [28].

#### **2.2.3.10. Drug loading efficiency**

For determining the IRB content, 1 mL of SNEDDS formulae (equivalent to 75 mg of IRB) was diluted with acidified methanol (1% V/V 0.1N HCl) and emulsified under moderate agitation. After complete emulsification, the volume was made up to 75 mL with acidified methanol (1mg/mL). From the above stock solution, 0.2 mL (200µg/ml) was withdrawn and diluted up to 10mL with acidified methanol (20µg/ml). Samples were prepared in triplicate and absorbance was measured at 246 nm using UV-Vis Spectrophotometer (Hitachi U-2900, Japan). Acidified methanol was used as a reference solution. The amount of IRB present in each formula was calculated from a calibration plot previously determined for IRB [29].

#### **2.2.3.11. In-vitro drug release studies**

The *in-vitro* drug release of IRB from the optimized SNEDDS formulae, pure drug and marketed product (Irbedrin®) was performed using USP dissolution apparatus type II (Erweka, DT 600, Germany). The dissolution medium consisted of 900 mL of freshly prepared simulated gastric fluid (0.1N HCl, pH 1.2, enzyme-free) maintained at 37±0.5°C and the paddle speed was set at 50 rpm. Hard gelatin capsules, size “000” filled with pre-concentrate (equivalent to 75mg Irbesartan) were tied to paddles using para film spring to prevent capsules from floating. Aliquots (5 mL) from the dissolution medium were withdrawn at regular time intervals (5, 10, 15, 30, 45, 60, 90 and 120 min) using a calibrated disposable syringe. The withdrawn samples were replaced by equal volumes of dissolution medium to maintain the volume and sink conditions constant. The samples were then filtered through a membrane filter (0.45µm, Whatmann) and drug concentration was obtained after proper dilutions via UV validated method at 246 nm using UV-Vis Spectrophotometer (Hitachi U-2900, Japan). All measurements were done in triplicate [29].

#### **2.2.4. Preparation of IRB loaded S-SNEDDS**

Based on the rank order performed for all conventional SNEDDS formulae depending on their characterization and evaluation tests, two optimized SNEDDS formulae were selected to be solidified by spray drying technique using Aerosil 200 as solid carrier. Briefly, SNEDDS formula and Aerosil 200 (1000mg) were suspended in 200 mL ethanol with continuous stirring until forming an isotropic mixture. The mixture was then kept at room temperature and equilibrating for 24h. The suspension was then spray dried using a Buchi mini spray dryer (Buchi, B-190, Switzerland) under the following conditions: inlet temperature, 60 °C; outlet temperature, 35°C; aspiration, 85%; feeding rate of the suspension, 5 mL/min [30].

### 2.2.5. Characterization of IRB loaded S-SNEDDS

#### 2.2.5.1. Micromeritic properties of S-SNEDDS

##### Angle of repose ( $\theta$ )

The angle of repose of S-SNEDDS was determined by funnel method. Accurately weighed sample were taken in a funnel. Height of the funnel was adjusted in such a way that the tip of the funnel just touches the apex of the heap of S-SNEDDS powder. The powder was allowed to flow through funnel freely onto the surface. The diameter of the powder cone was measured and angle of repose calculated using the following equation [31]:

$$\tan \theta = h/r$$

Where; h = height of the heap, r = radius of the heap

##### Bulk and tapped density

Both bulk density (BD) and tapped density (TD) were determined. A quantity of 2 g of S-SNEDDS was introduced into a 10 mL measuring cylinder. Initial volume was observed, and then the cylinder was allowed to fall under its own weight onto a hard surface from a height of 2.5 cm at 2 second intervals. The tapping was continued until no further change in volume was noted. Bulk density and tapped density were calculated using the following equations [32]:

$$\text{BD} = \text{Weight of powder} / \text{Bulk Volume}$$

$$\text{TD} = \text{Weight of powder} / \text{Tapped Volume}$$

##### Compressibility Index

The compressibility of the S-SNEDDS granules was determined by Carr's Compressibility Index as follow [33]:

$$\text{Carr's Compressibility Index (\%)} = [(TD-BD) / TD] \times 100$$

##### Hausner ratio

It is the ratio of tapped density to bulk density. It gives an idea about the flow characters of powder particles and can be calculated as follow [32]:

$$\text{Hausner ratio} = \text{TD} / \text{BD}$$

#### 2.2.5.2. Reconstitution properties of S-SNEDDS

Reconstituted S-SNEDDS were characterized for robustness to dilution and self-emulsification time as described for liquid SNEDDS.

#### 2.2.5.3. Scanning electron microscopy (SEM)

Scanning electron micrographs for IRB, Aerosil 200 and prepared S-SNEDDS formulae were taken using Scanning electron microscope (JEOL, JSM 50A, Japan) operating at 20 kV to study surface topography and globule size of S-SNEDDS. The samples were fixed on SEM stub and then coated with thin layer of platinum [33].

#### 2.2.5.4. Differential Scanning Calorimetry (DSC)

Physical state of IRB in S-SNEDDS was characterized using differential scanning calorimeter. Thermograms of IRB, Aerosil 200, physical mixture of both and prepared optimized S-SNEDDS formulae were obtained using differential scanning calorimeter (Shimadzu, DSC-50, Japan). The thermal behavior was studied by heating nearly 2 mg of samples in sealed aluminum pans under nitrogen gas flow (30 mL/min) over a temperature range of 0 to 250°C and a heating rate of 10°C/min [34].

#### 2.2.5.5. Fourier Transformed Infrared Spectroscopy (FTIR)

FTIR Spectra of pure IRB, Aerosil 200, physical mixture of both and prepared optimized S-SNEDDS formulae were obtained using Fourier transformed infrared spectrophotometer (Shimadzu 8400, Japan). Solid samples were mixed with small quantity of IR grade potassium bromide and compressed into discs by applying pressure. The compressed disc was placed in light path and the spectrum was obtained. Each KBr disc was scanned at 4 mm/s at a resolution of 2 cm over a wave number region of 4000–400  $\text{cm}^{-1}$  [35].

#### 2.2.5.6. Drug loading efficiency

IRB content in S-SNEDDS formulae was estimated using the method previously mentioned for liquid SNEDDS [28].

### 2.2.5.7. *In-vitro* drug release studies

The *in-vitro* drug release of IRB from the optimized S-SNEDDS formulae was performed using the above mentioned method for conventional liquid SNEDDS [29].

## RESULTS AND DISCUSSION

### 3.1. Preformulation Study (Selection of SNEDDS Components)

#### 3.1.1. Study of IRB solubility in various oils, surfactants and cosurfactants

To design a SNEDDS with acceptable physicochemical characteristics, the components of the system including oil phase, surfactant and cosurfactant must be carefully chosen. Solubility studies aimed at identifying suitable SNEDDS components that possess good solubilizing capacity for IRB. Identifying the suitable oil, surfactant and cosurfactant having maximal solubilizing potential for drug under investigation is very important to achieve optimum drug loading [36]. Oils can solubilize the lipophilic drug in a specific amount so they are the main excipients because they can increase the fraction of lipophilic drug transported via the intestinal lymphatic system, thereby increasing absorption from the GI tract. All the investigated oils were fatty acids commonly utilized in SNEDDS formulation that differ in nature and chain length [37]. Capryol 90 was selected as an oily phase for IRB due to its highest solubilization ( $176.47 \pm 5.48$  mg/mL) compared to other screened oils as shown in figure (2). This may be attributed to the medium chain length (eight carbons) and the amphiphilic nature of Capryol 90 which provide it with surfactant properties and therefore, enhance drug solubilization, as explained by Balakrishnan et al [38]. Besides its high drug solubilization power, Capryol 90 being a saturated medium chain fatty acid with HLB value = 6 is known for its efficient self-emulsification properties which aids the formation of the self-emulsifying system containing the drug [39]. All the investigated surfactants in this study were non-ionic hydrophilic ones. Being non-ionic, the investigated surfactants are considered safe and biocompatible [40] and being hydrophilic (with HLB values > 10), they are superior in forming fine, uniform emulsion droplets which can empty rapidly from the stomach and provide large surface area that facilitates rapid drug release and absorption. In addition, the chosen surfactants were reported for their bioactive properties that increase the intracellular concentration of the co-applied drug resulting in absorption enhancement [41]. Surfactants also form a layer around the emulsion droplets and hence reduce the interfacial energy, as well as provide a mechanical barrier to coalescence. This can prevent precipitation of the drug within the GI lumen and enhance prolonged existence of drug molecules. Among the various surfactants screened, Cremophor RH40 showed the best solubilizing potential for IRB ( $261.74 \pm 6.18$  mg/mL) as illustrated in figure (3). Transient negative interfacial tension and a fluid interfacial film are rarely achieved with the use of a single surfactant, usually necessitating the addition of a cosurfactant. The presence of cosurfactants decreases the bending stress of the interface and allows an interfacial film with sufficient flexibility to assume different curvatures required to form a nanoemulsion over a wide range of compositions. Hence the use of cosurfactant stabilizes the formed nanoemulsion. Among the different cosurfactants used in this study, Transcutol HP exhibited maximum solubility for IRB ( $287.56 \pm 6.67$  mg/mL) as presented in Figures (4). Similar results were obtained by Urvashi et al., who found that the optimized components for lovastatin SNEDDS are Capryol 90 as oil, Cremophor RH40 as surfactant and Transcutol HP as cosurfactant [42].

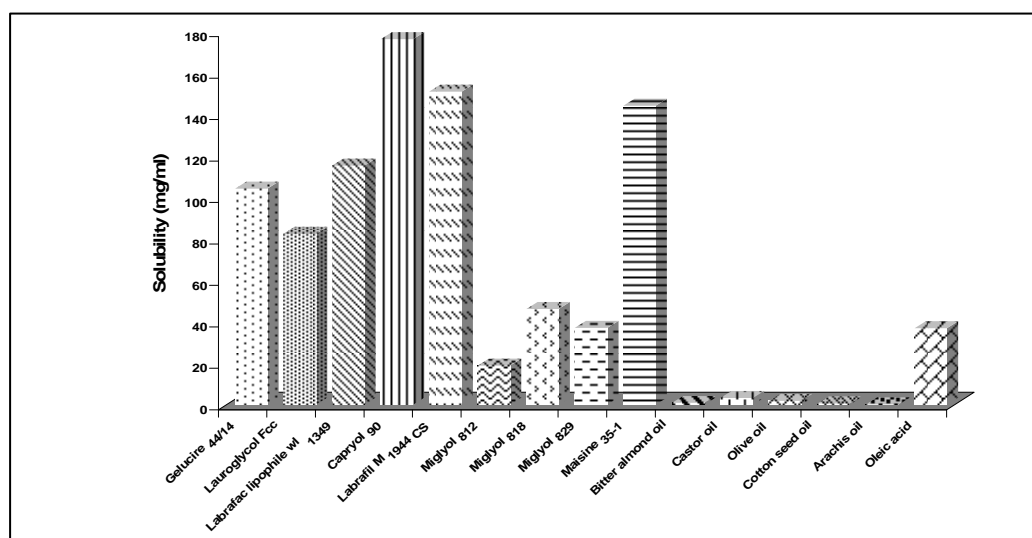


Fig. 2. Solubility of IRB in various oils

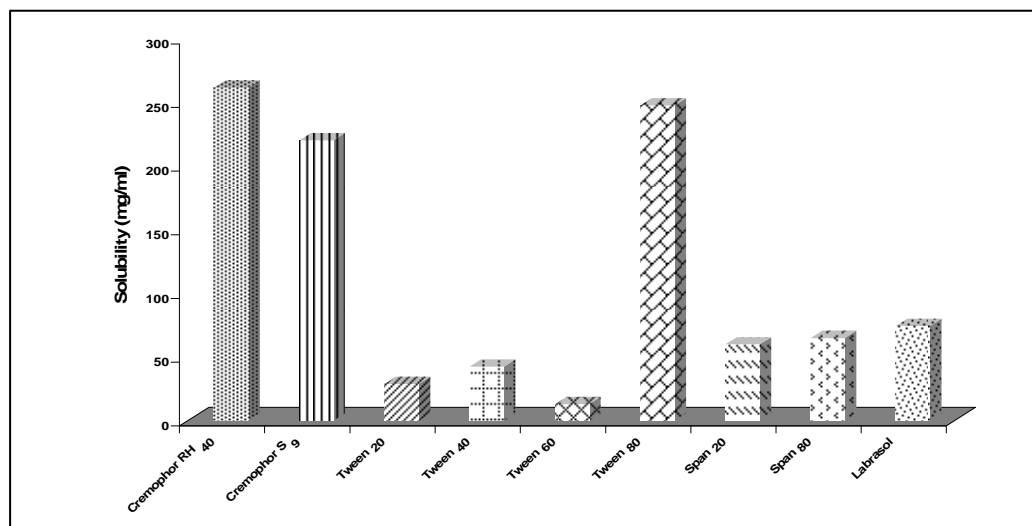


Fig. 3. Solubility of IRB in various surfactants

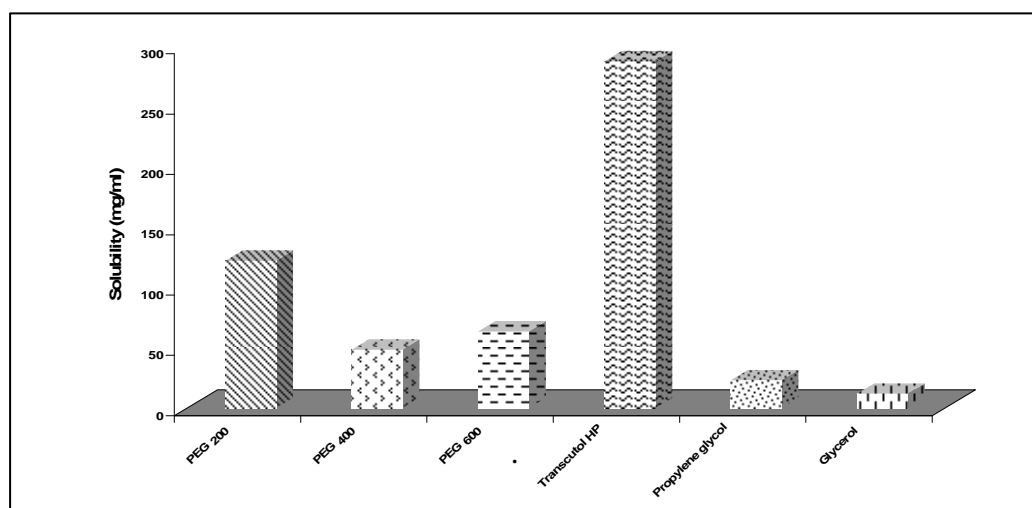


Fig. 4. Solubility of IRB in various cosurfactants

### 3.1.2. Preliminary screening of surfactants for emulsification efficiency

Although being a major parameter in choosing the ingredients of the SNEDDS, drug solubility is not the only parameter governing the choice of the surfactant in the prepared systems. The emulsifying efficiency of the surfactant is rather a much more important factor [43]. Therefore, the emulsifying efficiency of different surfactants was screened regarding the selected oil. The ability of the surfactant to form an emulsion was assessed by the number of flask inversions needed for emulsion formation, while the stability of the formed emulsion was expressed by its percent UV transmission, two hours after preparation. Optical clarity corresponds to high transmittance, as opalescent dispersions will scatter incident radiation to larger extent as compared to transparent dispersions. The intensity of light passing through such dispersion is attributed to the scattering of light which occurs due to absence of optical homogeneities in the medium [44]. Hence, percentage transmittance could directly be used to predict relative droplet size of the emulsion. Based on this principle, aqueous dispersions with high transmittance (lower absorbance) were considered optically clear and oil droplets were thought to be in a state of nanodispersion [45]. The percentage transmittance values and number of flask inversions of various dispersions are listed in table (2). For all screened surfactants, the largest number of flask inversions (17 inversions) was reported for Cremophor S9, indicating the most difficulty in emulsion formation. In addition, emulsions formed by Cremophor S9 had the least stability as indicated by the least percent UV transmission reported ( $14.90 \pm 0.66$  %). On the other hand, relatively few numbers of flask inversions (4 inversions) were needed for emulsion formation using Cremophor RH40 as emulsifying agents, moreover, the percent UV transmission of the formed emulsions (two hours after preparation) approached 100% indicating an accepted stability of the formed emulsions. Thus, Cremophor RH40 was chosen as surfactant for further investigation due to its better nanoemulsification efficiency. These observed differences in the emulsification efficiency of the investigated surfactants were attributed to the difference in their chain length and structure as explained by Lawrence in his study on microemulsions as drug delivery vehicles [46].

**Tab. 2. Emulsification efficiency of various surfactants**

| Surfactants           | % Transmittance*    | No. of inversions |
|-----------------------|---------------------|-------------------|
| <b>Cremophor RH40</b> | <b>99.47 ± 0.12</b> | <b>4</b>          |
| Cremophor S9          | 14.90 ± 0.66        | 17                |
| Tween 20              | 98.17 ± 0.40        | 5                 |
| Tween 40              | 80.97 ± 1.01        | 11                |
| Tween 60              | 74.93 ± 0.35        | 9                 |
| Tween 80              | 97.60 ± 0.26        | 15                |
| Span 20               | 52.67 ± 0.75        | 17                |
| Span 80               | 56.57 ± 0.50        | 13                |
| Labrasol              | 44.87 ± 0.95        | 7                 |

\*Values are expressed as mean ± S.D, n=3

### 3.1.3. Preliminary screening of cosurfactants for emulsification efficiency

All the cosurfactants employed in this study appeared to improve the emulsification ability of Capryol 90 and Cremophor RH40. It was documented that negative interfacial tension and fluid interfacial film is rarely achieved by the use of a single surfactant, usually necessitating the addition of a cosurfactant. The presence of cosurfactants decreases the bending stress of interface and allows the interfacial film sufficient flexibility to acquire different curvatures required to form nanoemulsion over a wide range of compositions [17]. Addition of a cosurfactant to the surfactant-containing formulation was reported to improve the dispersibility and drug absorption from formulation [37]. As depicted in table (3), Transcutol HP exhibited good emulsification efficiency with Capryol 90 and Cremophor RH 40 mixture, showing maximum transmittance (99.83±0.06%) and 3 inversions only compared to other employed cosurfactants. It was cleared that all the employed cosurfactants appeared to improve the emulsification ability of Cremophor RH40 and Capryol 90. Finally, based on the results of preliminary screening of IRB, a distinct system was selected consisting of Capryol 90 as oily phase ,Cremophor RH40 as surfactant and Transcutol HP as cosurfactant and detailed study of the system was performed using pseudoternary phase diagram.

**Tab. 3. Emulsification efficiency of various cosurfactants**

| Cosurfactants        | % Transmittance*    | No. of inversions |
|----------------------|---------------------|-------------------|
| PEG 200              | 99.33 ± 0.38        | 5                 |
| PEG 400              | 99.53 ± 0.12        | 4                 |
| PEG 600              | 94.43 ± 0.15        | 4                 |
| <b>Transcutol HP</b> | <b>99.83 ± 0.06</b> | <b>3</b>          |
| Propylene glycol     | 98.80 ± 0.26        | 7                 |
| Glycerol             | 99.20 ± 0.10        | 15                |

\*Values are expressed as mean ± S.D, n=3

### 3.1.4. Construction of pseudoternary phase diagram

One of the most important characteristics of SNEDDS is the change that occurs when the system is diluted (since it will be diluted by body fluids after administration), which may cause drug precipitation due to the loss of solvent capacity [47]. Therefore, Pseudoternary phase diagrams were constructed to identify self-nanoemulsifying regions and to select suitable concentrations of oil, surfactant and cosurfactant for the formulation of SNEDDS. Components used for construction of pseudoternary phase diagram are Capryol 90 (oil phase), Cremophor RH40 (surfactant), Transcutol HP (cosurfactant) and distilled water (aqueous phase). The phase diagrams were mapped at surfactant/cosurfactant ratios (1:0, 1:1, 1:2, 1:3, 2:1 and 3:1). The size of the nanoemulsion region in the diagrams was compared, the larger the size the greater the self-nanoemulsification efficiency. The nanoemulsion phase was identified as the area where clear and transparent formulae were obtained on dilutions based on visual inspection of samples. Pseudoternary phase diagrams showed that the zone of nanoemulsion (the grayish area) was largest in formulae prepared with Cremophor RH 40-Transcutol HP mixture (Smix) at 1:1 ratio as shown in figures (5-10). Thus, fixing the surfactant/cosurfactant ratio at 1:1 is a better choice from the stability point of view [48]. At Smix 1:1, and when cosurfactant was added with surfactant in equal amounts, a higher nanoemulsion region was observed, perhaps because of the further reduction of the interfacial tension and increased fluidity of the interface at Smix 1:1.

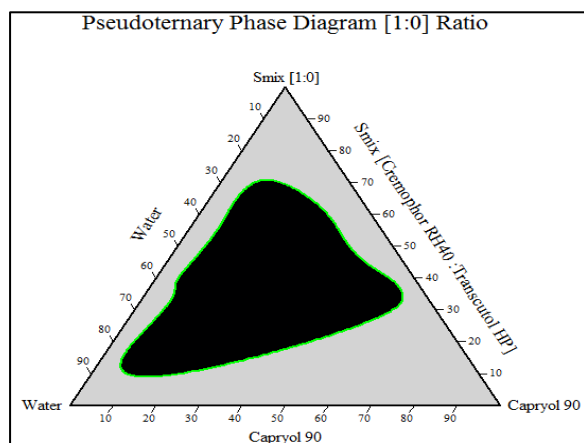


Fig. 5. Pseudo-ternary phase diagram of Smix [1:0]

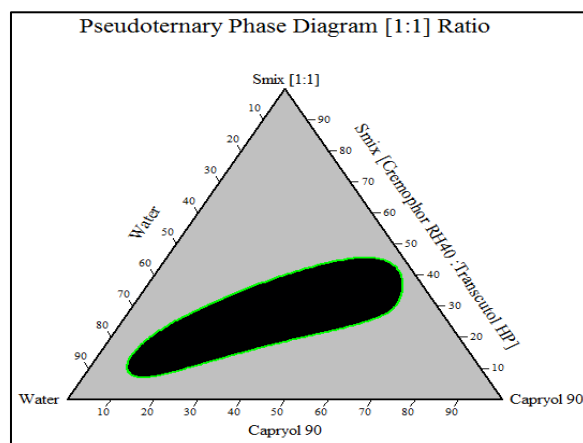


Fig. 6. Pseudo-ternary phase diagram of Smix [1:1]

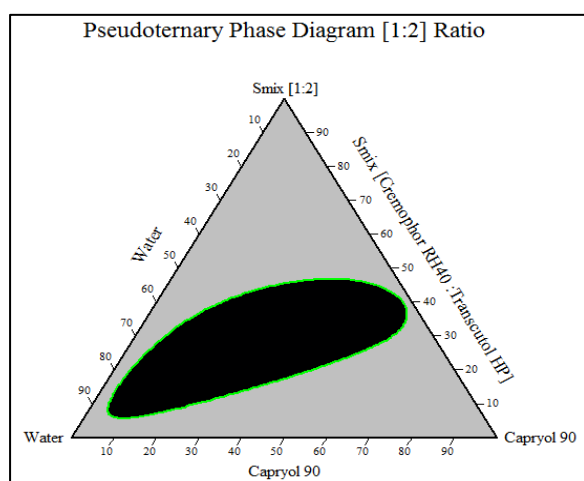


Fig. 7. Pseudo-ternary phase diagram of Smix [1:2]

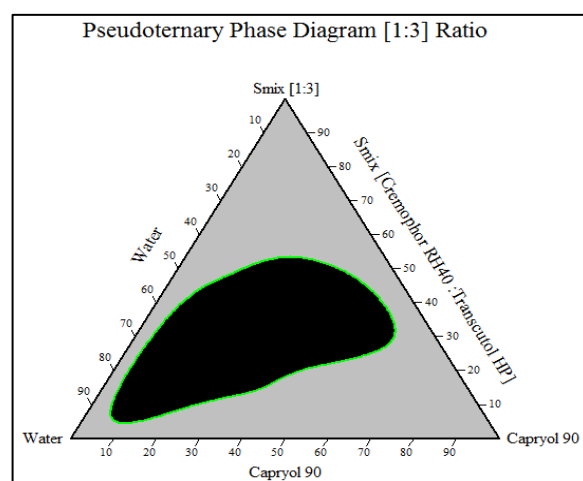


Fig. 8. Pseudo-ternary phase diagram of Smix [1:3]

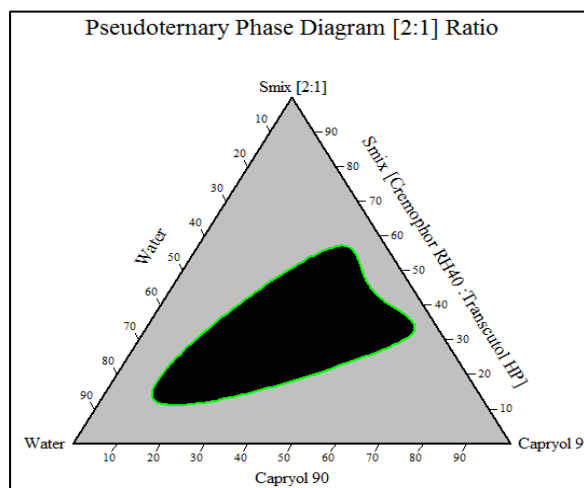


Fig. 9. Pseudo-ternary phase diagram of Smix [2:1]

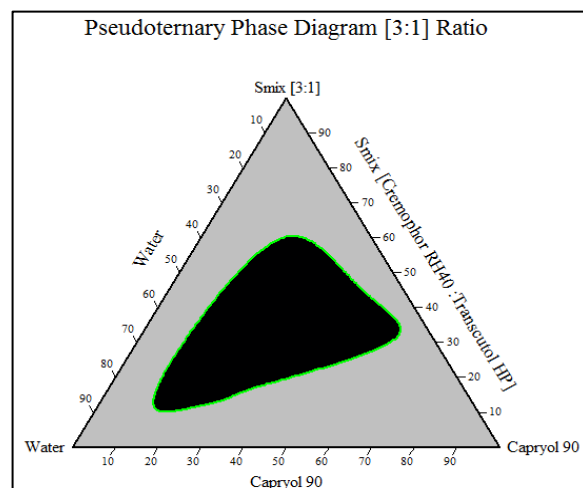


Fig. 10. Pseudo-ternary phase diagram of Smix [3:1]

### 3.2. Characterization and Evaluation of IRB loaded SNEDDS

#### 3.2.1. Thermodynamic stability studies

All IRB loaded SNEDDS formulae showed no signs of precipitation, cloudiness or separation after heating-cooling cycles, centrifugation and freeze-thaw cycles which ensured the stability of all reconstituted nanoemulsion. Visual observation indicated that there was no phase separation or any flocculation or precipitation in all formulae and the physical appearance of all formulae was similar. Thus, the overall stability of all SNEDDS formulae under these stress conditions was found to be acceptable. The observations found during thermodynamic stability studies are given in table (4). These results concur with those of Ashok et al., who prepared albendazole self-emulsifying drug

delivery system (SEDDS) and found that a sudden change in temperature had no effect in the entropy of the system [20].

**Tab. 4. Thermodynamic stability studies of various IRB loaded SNEDDS formulae**

| Formula | Heating cooling cycles | Centrifugation test | Freeze thaw cycles |
|---------|------------------------|---------------------|--------------------|
| F1      | √                      | √                   | √                  |
| F2      | √                      | √                   | √                  |
| F3      | √                      | √                   | √                  |
| F4      | √                      | √                   | √                  |
| F5      | √                      | √                   | √                  |
| F6      | √                      | √                   | √                  |
| F7      | √                      | √                   | √                  |
| F8      | √                      | √                   | √                  |

Where (√) indicates the formula passed the test.

### 3.2.2. Robustness to dilution

The ability of SNEDDS to be diluted without any phase separation and drug precipitation is essential for its use as a drug delivery vehicle since, after administration, it will almost certainly be diluted by body fluids. After dilution of all SNEDDS formulae, the resulting nanoemulsions were found to remain clear, transparent and showed no phase separation even after 24 hours as shown in table (5). This gave a good indication about the suitability of such systems for oral application where they have a great chance to pass along the gastrointestinal tract as emulsified oil globules without phase separation. This implied that all SNEDDS formulae loaded with IRB were stable at infinite aqueous dilution. In addition, the composition and pH of the aqueous phase was found to have no effect on the properties of nanoemulsions [49]. Similar results were reported by Anuradha *et al.*, who formulated Peppermint oil based drug delivery system of aceclofenac and found that after dilution, the resulting microemulsions were found to remain clear, transparent and appeared like homogenous single-phase liquids [44].

**Tab. 5. Robustness to dilution results of various IRB loaded SNEDDS formulae**

| Formula | Distilled Water |     |      | 0.1 N HCL |     |      | Phosphate Buffer pH 6.8 |     |      |
|---------|-----------------|-----|------|-----------|-----|------|-------------------------|-----|------|
|         | 10              | 100 | 1000 | 10        | 100 | 1000 | 10                      | 100 | 1000 |
| F1      | √               | √   | √    | √         | √   | √    | √                       | √   | √    |
| F2      | √               | √   | √    | √         | √   | √    | √                       | √   | √    |
| F3      | √               | √   | √    | √         | √   | √    | √                       | √   | √    |
| F4      | √               | √   | √    | √         | √   | √    | √                       | √   | √    |
| F5      | √               | √   | √    | √         | √   | √    | √                       | √   | √    |
| F6      | √               | √   | √    | √         | √   | √    | √                       | √   | √    |
| F7      | √               | √   | √    | √         | √   | √    | √                       | √   | √    |
| F8      | √               | √   | √    | √         | √   | √    | √                       | √   | √    |

Where (√) means stable formula which showed no phase separation or precipitation

### 3.2.3. Assessment of efficiency of self-emulsification (Dispersibility test)

The *in-vitro* performances of the formulae were visually assessed using the grading system previously mentioned and the results were shown in table (6). Visual observations showed that all SNEDDS formulae were found to be grade A. The rapid self-emulsification of the investigated systems can be attributed to their low oil content (5-11.5%w/w). This ability is very important for efficient SNEDDS as emulsification process is considered the rate limiting process for drug absorption. Similar observations were reported by Naseem *et al.*, who prepared self-nanoemulsifying lipid carrier system of Etoposide and found that six formulations were robust to exist in nanoemulsion form upon dispersion in the simulated aqueous environments of the GI tract and categorized them as grade (A) [25].

**Tab. 6. Visual observations of dispersibility test for various IRB loaded SNEDDS formulae**

| Formula | Observations                   | Grade |
|---------|--------------------------------|-------|
| F1      | Rapidly forming clear emulsion | A     |
| F2      | Rapidly forming clear emulsion | A     |
| F3      | Rapidly forming clear emulsion | A     |
| F4      | Rapidly forming clear emulsion | A     |
| F5      | Rapidly forming clear emulsion | A     |
| F6      | Rapidly forming clear emulsion | A     |
| F7      | Rapidly forming clear emulsion | A     |
| F8      | Rapidly forming clear emulsion | A     |

### 3.2.4. Self-emulsification time

The rate of emulsification is an important index for the assessment of the emulsification efficiency of SNEDDS. Since the free energy required to form a nanoemulsion is very low, the formation is thermodynamically

spontaneous. The SNEDDS should disperse completely and quickly when subjected to aqueous dilution under mild agitation. The recorded self-emulsification times for the eight tested IRB loaded formulae are represented in table (7). From the results obtained, it was evident that all the tested formulae were self-emulsified within  $11.23 \pm 1.70$  to  $19.05 \pm 1.21$  seconds. The short self-emulsification time reported for all the investigated systems indicate their ability for easy and rapid emulsification. The results revealed that self-emulsification time depends mainly upon the individual composition and its proportion of oil, surfactant and cosurfactant. From the self-emulsification time results, it was remarked that as the concentration of surfactant increases, the spontaneity of emulsification process increased and self-emulsification time decreases. This may be due to capacity of Cremophor RH40 in reducing the interfacial tension and thus excess diffusion of aqueous phase into the oil occur causing significant interfacial disruption and discharge of droplet into the bulk aqueous phase [50].

### 3.2.5. Viscosity determination

Viscosity studies are necessary for SNEDDS to characterize the system physically and to control its stability. The viscosity of SNEDDS is critical during their dispersion in the aqueous phase. Higher viscosities tend to slow down the emulsification rate which may affect *in-vivo* drug release and bioavailability profiles. From viscosity determination results, it was observed that as the concentration of oil and  $S_{mix}$  increased the viscosity of SNEDDS formulae also get increased as shown in figure (11). The IRB SNEDDS formulae had the average viscosity range between  $19.26 \pm 1.91$  cps and  $51.62 \pm 0.47$  cps. However after dilution with 100 times distilled water, the viscosity range decrease and became between  $7.90 \pm 0.43$  cps and  $27.93 \pm 0.96$  cps. All formulae were found to have rather low viscosities which indicated the resulted nanoemulsion to be O/W type. The viscosity values recorded by the SNEDDS formulae in the present study were low enough to preclude the possibility of rapid self-emulsification [51].

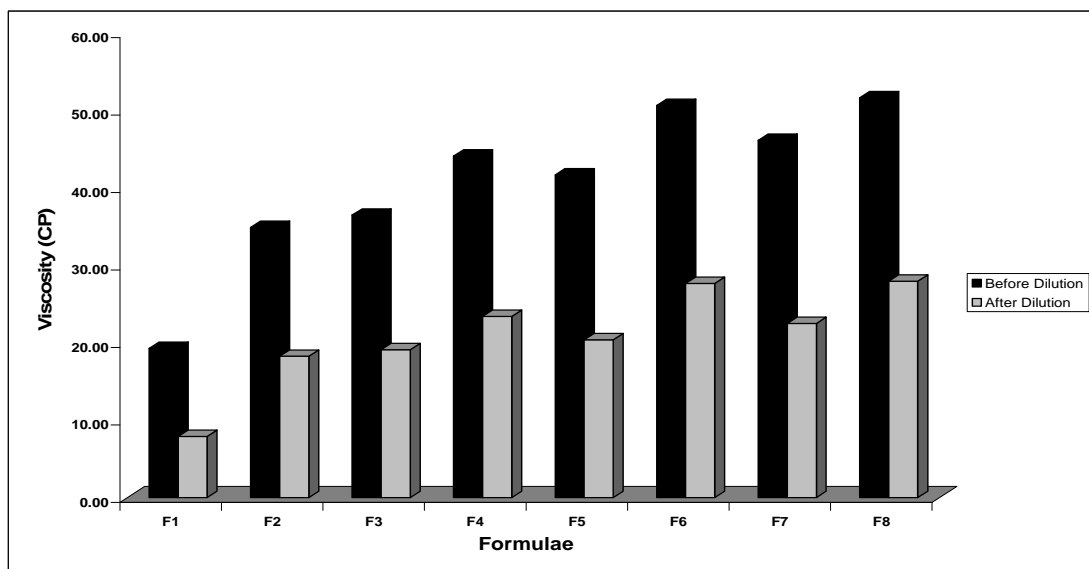


Fig. 11. Plot of viscosity before and after dilution for various IRB loaded SNEDDS formulae

### 3.2.6. Spectroscopic characterization of optical clarity

The percentage transmittance is an important parameter to determine the isotropic nature of the system. A value of percent transmittance closer to 100% signified that all selected formulae were clear, transparent and globules size in the nanometric range, which in turn indicates that the formula has a large surface area for drug release, high capacity to undergo enhanced absorption in biological matrix and thus have ability for increased oral bioavailability. Higher transmittance should be obtained with optically clear solutions, since cloudier solutions will scatter more of the incident radiation, resulting in lower transmittance. On 100 fold dilution, the percentage transmittance of SNEDDS formulae was found to be in the range of 98.40 % to 99.83 % as presented in table (7) which confirms good transparent nature of all IRB loaded SNEDDS formulae. These results are in agreement with the results reported by Naseem *et al.*, who found that the percentage transmittance of the prepared SNEDDS formulae were close to 100% [25].

### 3.2.7. Transmission electron microscopy (TEM)

TEM photographs of IRB loaded SNEDDS formulae subsequent to post dilution with distilled water are shown in figures (12-19) and interpreted for surface morphology and globule size. From the presented figures, it was apparent that globules of all formulae were well dispersed and no globule aggregation took place. TEM analysis revealed the

formation of spherical and homogeneous droplets with a size smaller than 50 nm, which satisfies the criteria of nanometric size range required for nanoemulsifying formulae [52].

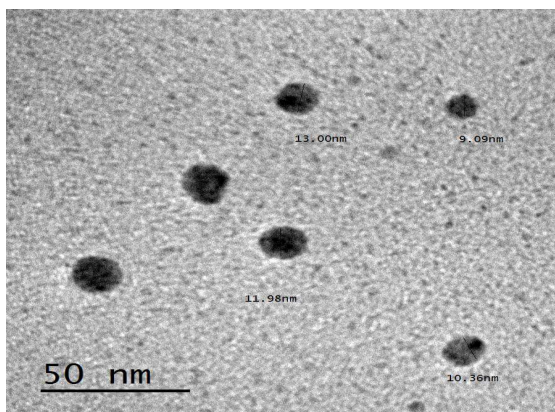


Fig. 12. TEM photograph of F1

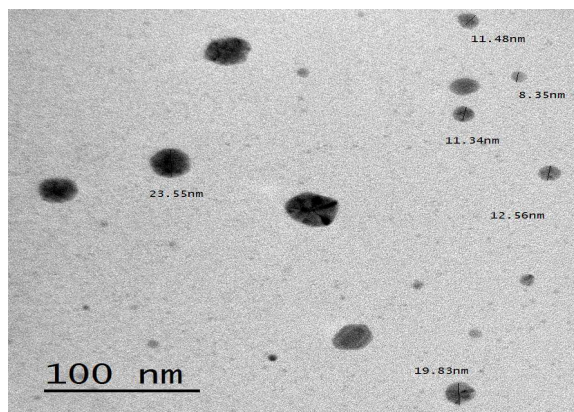


Fig. 13. TEM photograph of F2

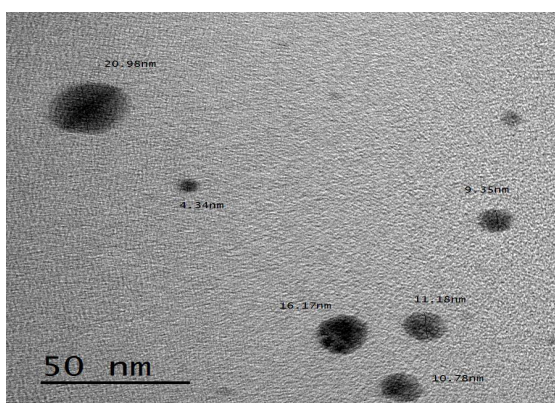


Fig. 14. TEM photograph of F3

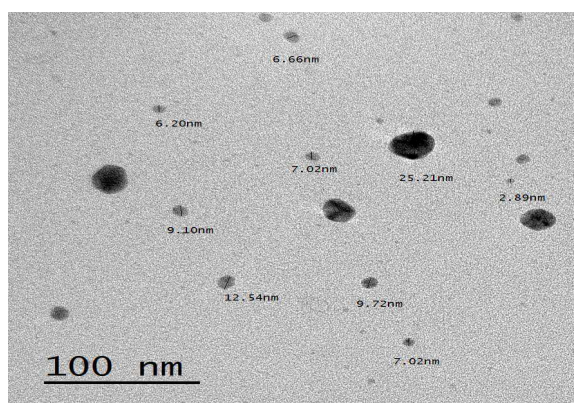


Fig. 15. TEM photograph of F4

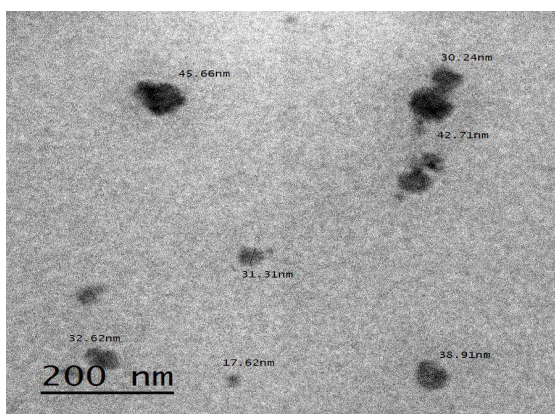


Fig. 16. TEM photograph of F5

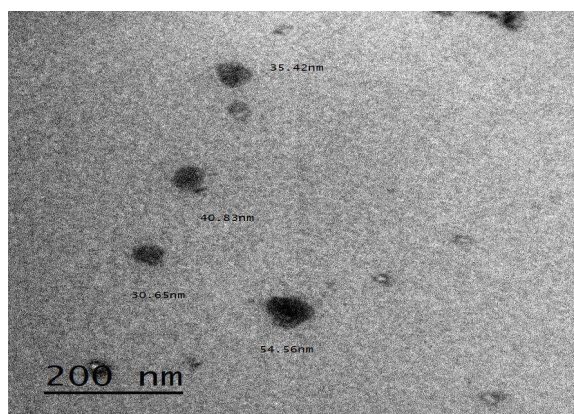


Fig. 17. TEM photograph of F6

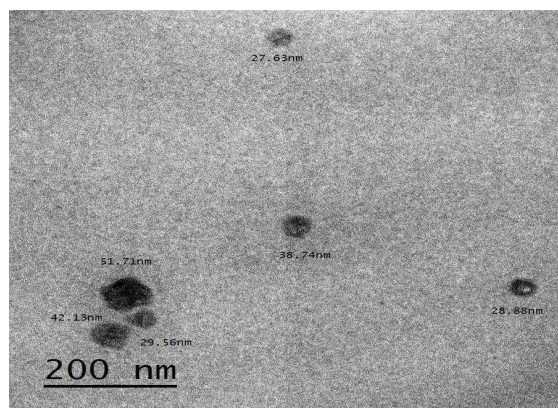


Fig. 18. TEM photograph of F7

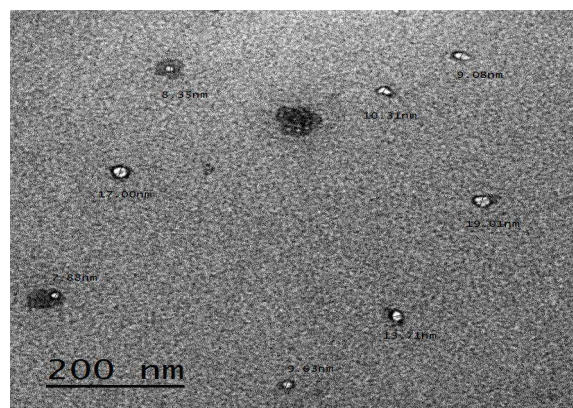


Fig. 19. TEM photograph of F8

### 3.2.8. Droplet size analysis and polydispersibility Index (PDI) determination

The droplet size is the crucial factor in the SNEDDS performance because it determines the rate and extent of drug release as well as drug absorption. Moreover, it has been reported that the smaller the particle size, the larger the interfacial surface area which may lead to more rapid absorption and improve the bioavailability. Systems with mean droplet size below 200 nm fulfill the criteria of SNEDDS. All the investigated systems had mean globule size less than 40 nm indicating their efficiency as SNEDDS. The small globule size of the diluted systems can be attributed to the use of the proper surfactant/cosurfactant mixture. This provided adequate reduction in the free energy of the system which in turn resisted the thermodynamic instabilities on changing the environment pH and volume. Also, the surfactant/cosurfactant mixture provided a strong mechanical barrier to protect the formed globules from being aggregated as explained by Nepal *et al* [53] and Singh *et al* [54]. From droplet size analysis it was observed that IRB loaded SNEDDS formulae had the mean particle size in the range of 15.77 to 32.22 nm indicating their efficiency as SNEDDS as shown in figures (20-27). It was also noticed that as the surfactant percentage increased, the mean droplet size decreased [55]. Furthermore, the droplet size increased when the concentration of lipid added increased from 5% to 11.5% due to the simultaneous decrease in the  $S_{mix}$  proportions [56]. The decrease in droplet size may be due to more surfactant being available for adsorption and the formation of a more closely packed surfactant film at the oil–water interface, thereby providing stable and condense interfacial film, as well as the low interfacial tension in the system. The mean droplet size is not the only parameter to be considered in the formulation of SNEDDS. The droplet size distribution is another parameter of equal importance. The droplet size distribution is expressed by a dimensionless value called the polydispersibility index (PDI) which is the measure of particle homogeneity and it varies from 0.0 to 1.0. The closer to zero the PDI value, the more homogenous are the particles. The small values of PDI shown by all SNEDDS formulae (0.057-0.315) indicate homogenous droplet population and narrow globule size distribution as reported in table (7). This in turn indicates more uniform emulsions with higher physical stability.

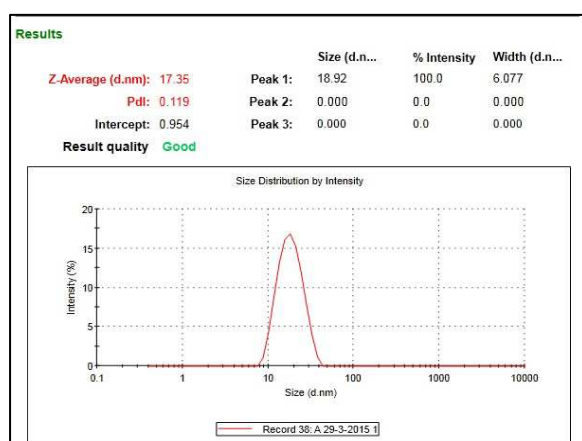


Fig. 20. Droplet size analysis of F1

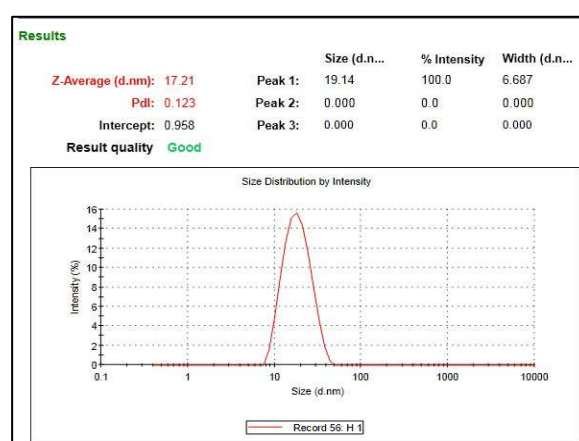


Fig. 21. Droplet size analysis of F2

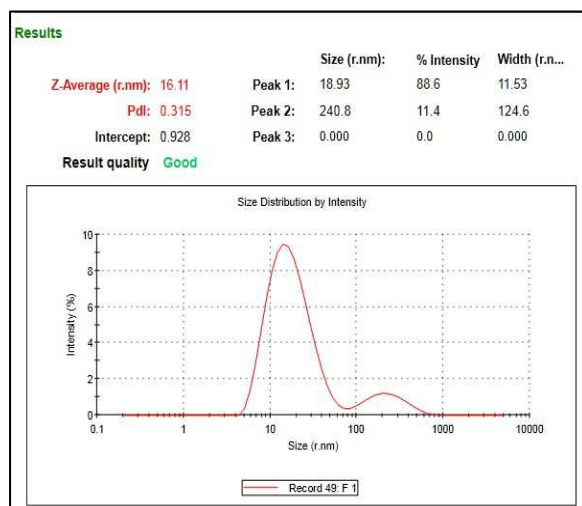


Fig. 22. Droplet size analysis of F3

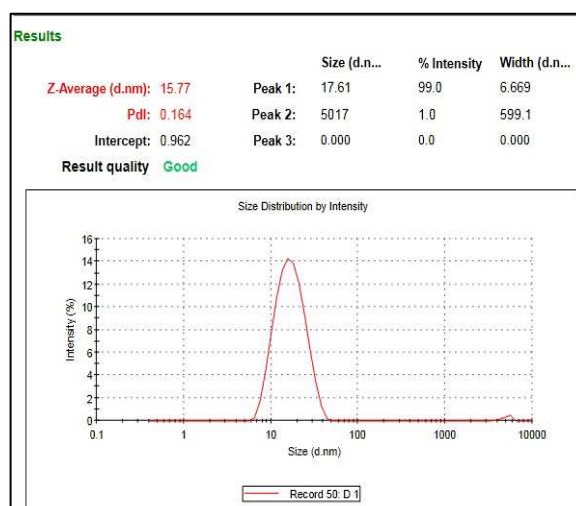


Fig. 23. Droplet size analysis of F4



Fig. 24. Droplet size analysis of F5

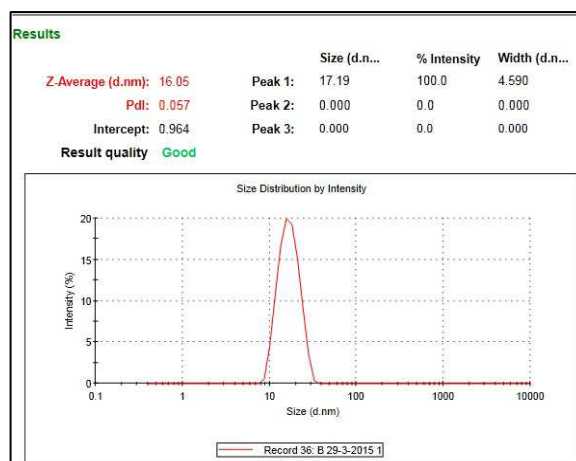


Fig. 25. Droplet size analysis of F6

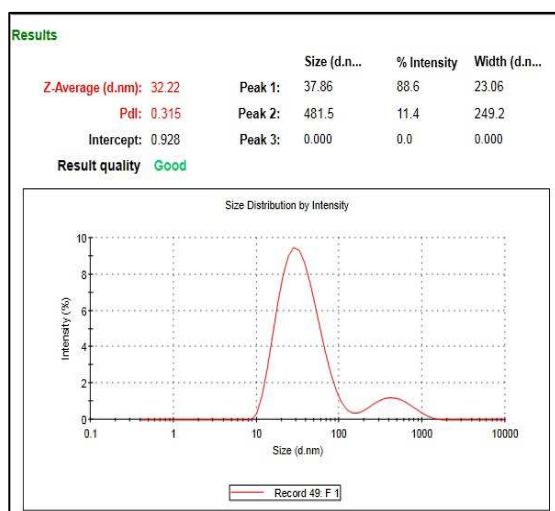


Fig. 26. Droplet size analysis of F7

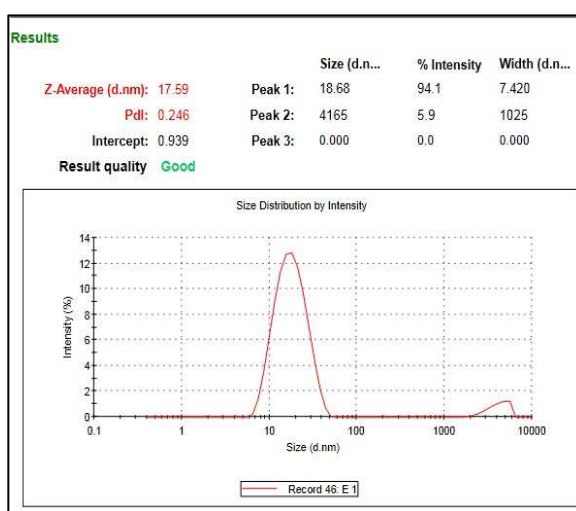


Fig. 27. Droplet size analysis of F8

### 3.2.9. Zeta potential determination

The zeta potential values of IRB loaded SNEDDS formulae are listed in table (7). The results were in the range of -3.19 to -11.30 mV. Negative values of zeta potential of all formulae give indication of stable systems [57]. Our

results were in complete accordance with Maulik et al. who prepared stable SMEDDS lovastatin oral formulations, and found that Zeta potential of all SNEDDS formulae was found between -0.228 to -10.7 mV, that may be due to that formulation consist of non-ionic components which show relatively neutral charge and not affected by body membrane charge during absorption [58].

### 3.2.10. Drug loading efficiency

The drug loading efficiency of all SNEDDS formulae was found in the range of  $94.08 \pm 1.66$  for F1 to  $99.84 \pm 0.95$  % for F8, indicating uniform drug dispersion in formulae as shown in table (7). Statistically it was further justified that there was no significant difference in drug content among the various formulae. It was also observed that the formulae F5 and F8 have the highest drug content. This may be attributed due to higher concentration of surfactant and cosurfactant in these two formulae that possess high solubilization capacity to solubilize the 75 mg dose of IRB. These observations are in line with studies reported by Ashish et al. who found that the drug content of Furosemide SNEDDS in between  $90.08 \pm 0.124$  and  $102.45 \pm 0.312$  [59].

Tab. 7. Self-emulsification time, % Transmittance, PDI, zeta potential and drug loading efficiency of IRB

| Formula | Self-emulsification Time* (Sec.) | % Transmittance* | PDI   | Zeta Potential (mV) | Drug Loading Efficiency* (%) |
|---------|----------------------------------|------------------|-------|---------------------|------------------------------|
| F1      | $19.05 \pm 1.21$                 | $99.47 \pm 0.06$ | 0.119 | -11.3               | $94.08 \pm 1.66$             |
| F2      | $16.63 \pm 1.31$                 | $99.73 \pm 0.12$ | 0.123 | -3.57               | $97.24 \pm 1.04$             |
| F3      | $12.27 \pm 1.16$                 | $99.40 \pm 0.10$ | 0.315 | -5.02               | $98.42 \pm 0.91$             |
| F4      | $11.23 \pm 1.70$                 | $99.83 \pm 0.12$ | 0.164 | -3.37               | $96.82 \pm 1.17$             |
| F5      | $17.06 \pm 0.68$                 | $98.63 \pm 0.15$ | 0.111 | -4.09               | $99.09 \pm 0.49$             |
| F6      | $14.09 \pm 1.69$                 | $99.07 \pm 0.21$ | 0.057 | -3.19               | $98.06 \pm 0.69$             |
| F7      | $17.78 \pm 0.60$                 | $98.40 \pm 0.26$ | 0.315 | -4.46               | $98.70 \pm 0.87$             |
| F8      | $16.85 \pm 1.38$                 | $98.90 \pm 0.20$ | 0.246 | -4.93               | $99.84 \pm 0.95$             |

\*Values are expressed as mean  $\pm$  S.D, n=3

### 3.2.11. In-vitro drug release studies

The dissolution profiles of different IRB SNEDDS formulae together with the dissolution profile of pure IRB filled in hard gelatin capsules, and that of IRB marketed tablets (Irbedrin®) are presented in Figure (28). Also, no dissolution-accelerating components or surfactants, such as sodium lauryl sulfate, were added to the media, because these components result in failure to discriminate between different dissolution profiles as the surfactant is the key element in improving dissolution of SNEDDS dosage forms [60]. Figure (28) signifies that dissolution profiles of IRB from SNEDDS formulae produced constantly superior drug dissolution rate as compared to that of pure drug and that of marketed tablets (Irbedrin®). Within the initial one hour of the dissolution study, only  $9.73 \pm 0.54\%$  and  $43.34 \pm 1.49\%$  of IRB was dissolved from pure powder and marketed tablets, respectively; Whereas, the SNEDDS formulae showed improved release within the same time period where more than 90% of IRB was released from formulae F3, F4, F5 and F7. IRB dissolved and released from SNEDDS reached  $97.03 \pm 2.82\%$  for formula F3,  $93.14 \pm 2.27\%$  for formula F4,  $100.52 \pm 2.88\%$  for formula F5 and  $96.28 \pm 0.78$  for formula F7 within one hour. This enhancement in IRB dissolution rate and extent could be attributed to the spontaneous formation of nanoemulsion during dissolution process with droplet size in nanometric range induced the presentation of IRB at dissolved state in the form of nanoemulsion which lead to an increased solubilization and enhanced drug dissolution rate and extent. Thus, this greater availability of dissolved IRB from the SNEDDS formulae could lead to higher absorption and higher oral bioavailability. In contrast to this, the release of IRB from formulae F6 and F8 were significantly lower than from other formulae, which may be attributed to the higher percentage of surfactants employed in these two formulae resulting in higher probability of surfactant migration into surrounding aqueous media upon dispersion. This process leads to formation of micelles that traps the free drug creating hindrances in drug release [61]. This indicates that the release of IRB from SNEDDS varied with respect to the concentration and O/Smix ratio. Also, the comparatively slow IRB dissolution from pure powder and the marketed tablets can mainly be explained by the poor water solubility of the drug [13,23]. This finding also supported the hypothesis that nano-sized droplets of emulsion can enhance the release of poorly soluble drugs [62]. It was also observed that there was a good correlation between the droplet size of generated nanoemulsions after reconstitution of SNEDDS and the dissolution rate of IRB. In another words, the amount of drug dissolved in the aqueous phase at time t, is inversely proportional to the droplet size of the generated nanoemulsions after SNEDDS reconstitution [18]. Thus, this rapid drug release was promoted by the larger interfacial areas present in emulsions with smaller drops [9]. Finally, the *in vitro* dissolution studies indicate that formulation of IRB in the form of SNEDDS formulation enhances the dissolution properties.

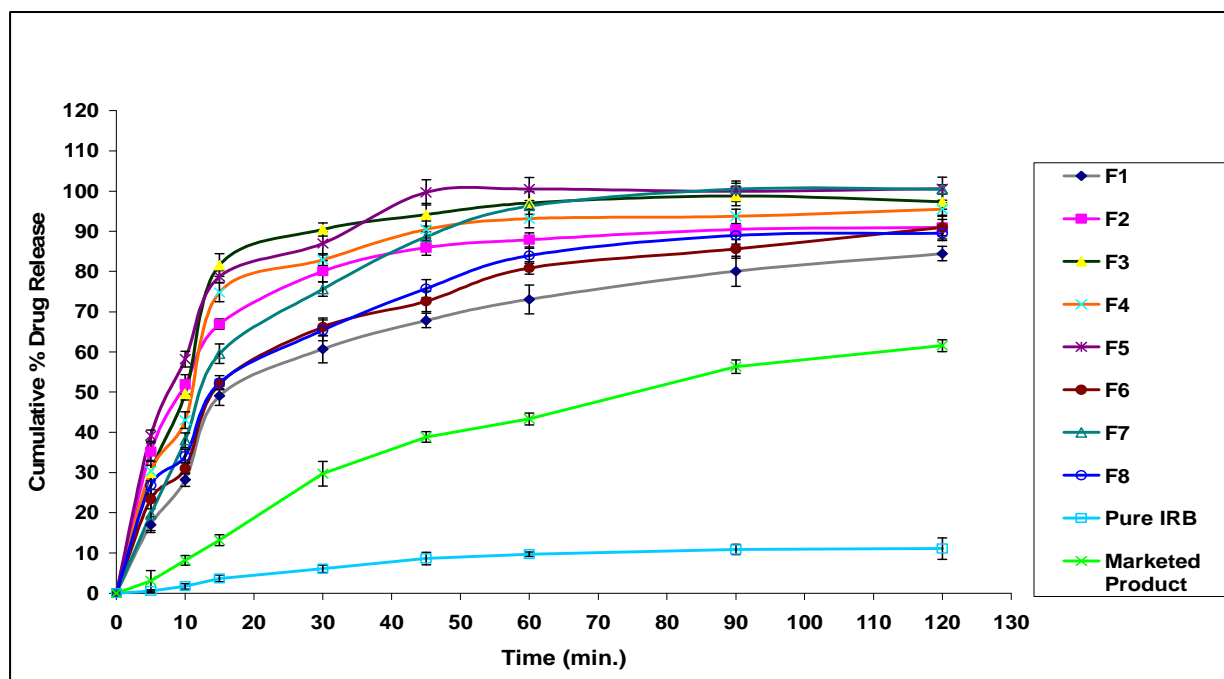


Fig. 28. *In-vitro* release profiles of IRB SNEDDS formulae compared with pure IRB and marketed product

### 3.3. Preparation of IRB loaded S-SNEDDS

Based on the rank order performed for all conventional SNEDDS formulae depending on their characterization and evaluation tests, two optimized SNEDDS formulae were selected to be converted into S-SNEDDS. From the *in-vitro* drug release data, drug loading efficiency and particle size analysis formulae F3 and F5 were selected as optimized formulae to be solidified into S-SNEDDS as illustrated in table (8).

Tab. 8. Rank order of conventional SNEDDS formulae according to *in-vitro* drug release data, drug loading efficiency and particle size analysis

| Formula | <i>In-vitro</i> drug release (1 hr) | Drug loading efficiency | Particle Size | Total rank order | Conclusive rank order |
|---------|-------------------------------------|-------------------------|---------------|------------------|-----------------------|
| F1      | 8                                   | 8                       | 5             | 21               | 8                     |
| F2      | 5                                   | 6                       | 4             | 15               | 7                     |
| F3      | 2                                   | 4                       | 3             | 9                | 1                     |
| F4      | 4                                   | 7                       | 1             | 12               | 3                     |
| F5      | 1                                   | 2                       | 7             | 10               | 2                     |
| F6      | 7                                   | 5                       | 2             | 14               | 5                     |
| F7      | 3                                   | 3                       | 8             | 14               | 5                     |
| F8      | 6                                   | 1                       | 6             | 13               | 4                     |

### 3.4. Characterization of IRB loaded S-SNEDDS

#### 3.4.1. Micromeritic properties of S-SNEDDS

The values obtained for the angle of repose of the two S-SNEDDS formulae F3 and F5 were  $28.28^{\circ} \pm 0.18$  and  $26.01^{\circ} \pm 0.55$  respectively, as shown in table (9). These values indicate that all formulae have good flowability. The bulk density of the two formulae F3 and F5 was found to be  $0.51 \pm 0.01$  g/mL and  $0.53 \pm 0.01$  g/mL respectively. However, tapped density was  $0.61 \pm 0.01$  g/mL for formula F3 and  $0.58 \pm 0.01$  g/mL for formula F5. Carr's index of formulae F3 and F5 was found to be  $15.39 \pm 0.39$  and  $9.74 \pm 1.61$  respectively which give an indication about the good flowability of the two S-SNEDDS formulae. This was further supported by the values of Hausner's ratio. The results of Hausner ratio of formulae F3 and F5 were  $1.18 \pm 0.01$  and  $1.11 \pm 0.02$  respectively. The improved flowability of S-SNEDDS formulae may be due to good sphericity of particles.

Tab. 9. Micromeritic properties of IRB loaded S-SNEDDS

| Formula               | F3                       | F5                       |
|-----------------------|--------------------------|--------------------------|
| Angle of Repose       | $28.28^{\circ} \pm 0.18$ | $26.01^{\circ} \pm 0.55$ |
| Bulk Density (g/mL)   | $0.51 \pm 0.01$          | $0.53 \pm 0.01$          |
| Tapped Density (g/mL) | $0.61 \pm 0.01$          | $0.58 \pm 0.01$          |
| Carr's index (%)      | $15.39 \pm 0.39$         | $9.74 \pm 1.61$          |
| Hausner's ratio       | $1.18 \pm 0.01$          | $1.11 \pm 0.02$          |

### 3.4.2. Reconstitution properties of S-SNEDDS

Dilution study was done to observe the effect of dilution on S-SNEDDS, because dilution may better mimic the condition of stomach after oral administration. It was observed that the two S-SNEDDS formulae F3 and F5 disperse quickly and completely when subjected to aqueous environment under mild agitation. The two formulae showed spontaneous nanoemulsification and there was no sign of phase separation or phase inversion of nanoemulsion after storage of 24h. The efficiency of self-emulsification can also be estimated by measuring the emulsification time. The emulsification time was  $40.03 \pm 1.53$  s for formula F3 and  $36.68 \pm 2.66$  s for formula F5. It was also noticed that the emulsification times for liquid SNEDDS and S-SNEDDS were very close to each others, indicating that the spray-drying process did not have a remarkable influence on the emulsification performance of S-SNEDDS. These results were in complete accordance with Chun Chao *et al.* who prepared solid lipid-based self-emulsifying drug delivery system of agaricoglycerides and found that the spray-drying had no effect on the emulsification performance [63].

### 3.4.3. Scanning electron microscopy (SEM)

The surface morphology of pure IRB powder, Aerosil 200 and S-SNEDDS formulae of IRB was determined using scanning electron microscope as shown in figures (29-32). The IRB powder appeared with an irregular crystalline shape as needle shaped crystals having rough surfaces, its particle size varied in a wide range from less than  $1 \mu\text{m}$  to larger than dozens of micrometers. Aerosil 200 appears to be spherical porous particles of size of approximately  $10 \mu\text{m}$ . The image of the solid SNEDDS containing IRB, however, illustrate that the particles had the same outer macroscopic morphology consisting of well separated spherical particles with relatively deep dents and similar diameters. Following spray drying, the crystalline IRB turned out to be highly amorphous in nature. Crystalline structures characteristic of IRB are not seen in S-SNEDDS micrographs suggesting that the drug is present in a completely dissolved state in the Solid SMEDDS.

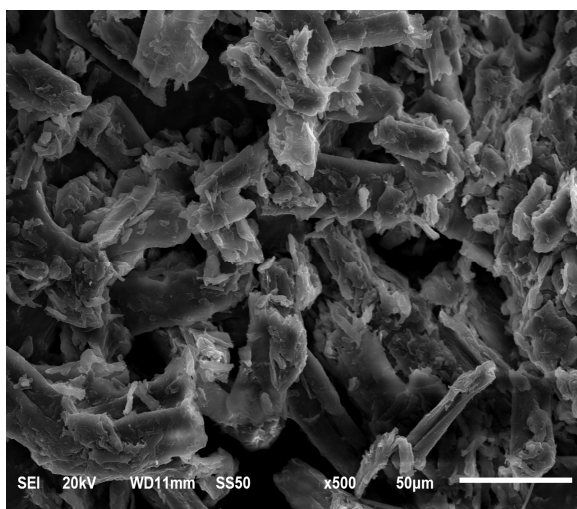


Fig. 29. SEM photograph of pure IRB

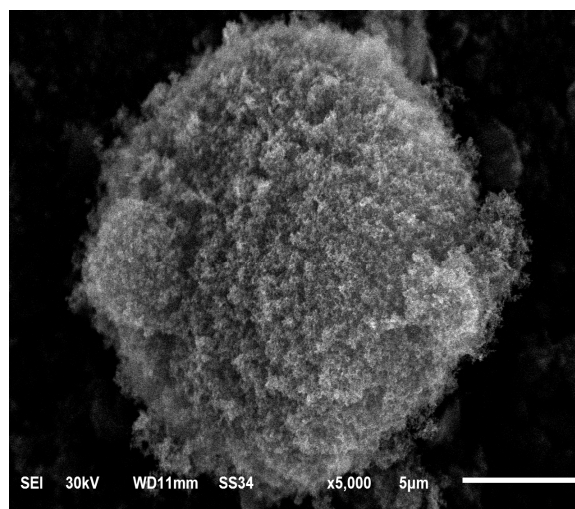


Fig. 30. SEM photograph of Aerosil

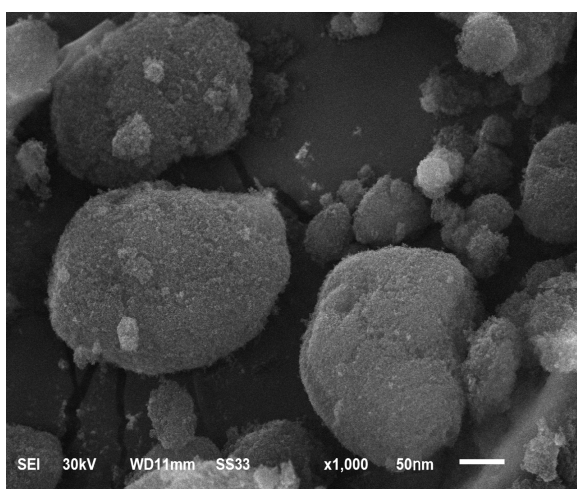


Fig. 31. SEM photograph of S-SNEDDS (F3)

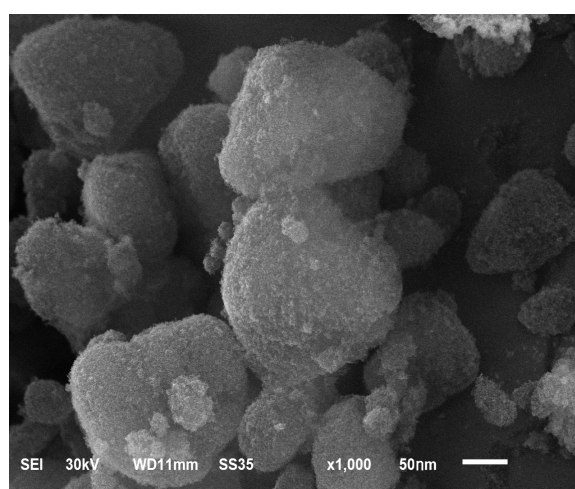


Fig. 32. SEM photograph of S-SNEDDS (F5)

#### 3.4.4. Differential Scanning Calorimetry (DSC)

Thermograms of pure IRB, Aerosil 200, physical mixture of both and prepared optimized S-SNEDDS formulae (F3 and F5) were obtained using differential scanning calorimeter as shown in figures (33-34). The thermogram of pure IRB exhibited a sharp endothermic peak at about 185.02 °C, corresponding to its melting point. Aerosil 200 showed no specific peaks from 0 to 250 °C as presented in figure (33). However, a melting endotherm having the characteristic peak of IRB was observed in the physical mixture of IRB and Aerosil 200. In the case of IRB S-SNEDDS formulae (F3 and F5), the endothermic peak of the drug was absent as shown in figures (33-34). The change in melting behavior of IRB can be attributed to the inhibition of its crystallization and solubilization of IRB in S-SNEDDS. Therefore, it could be concluded that IRB in the solid SNEDDS was in the amorphous form. It is known that transforming the physical state of a drug to the amorphous or partially amorphous state leads to a high-energy state and high disorder, resulting in enhanced solubility [30]. As a result, it was expected that the solid particles would also have enhanced solubility.

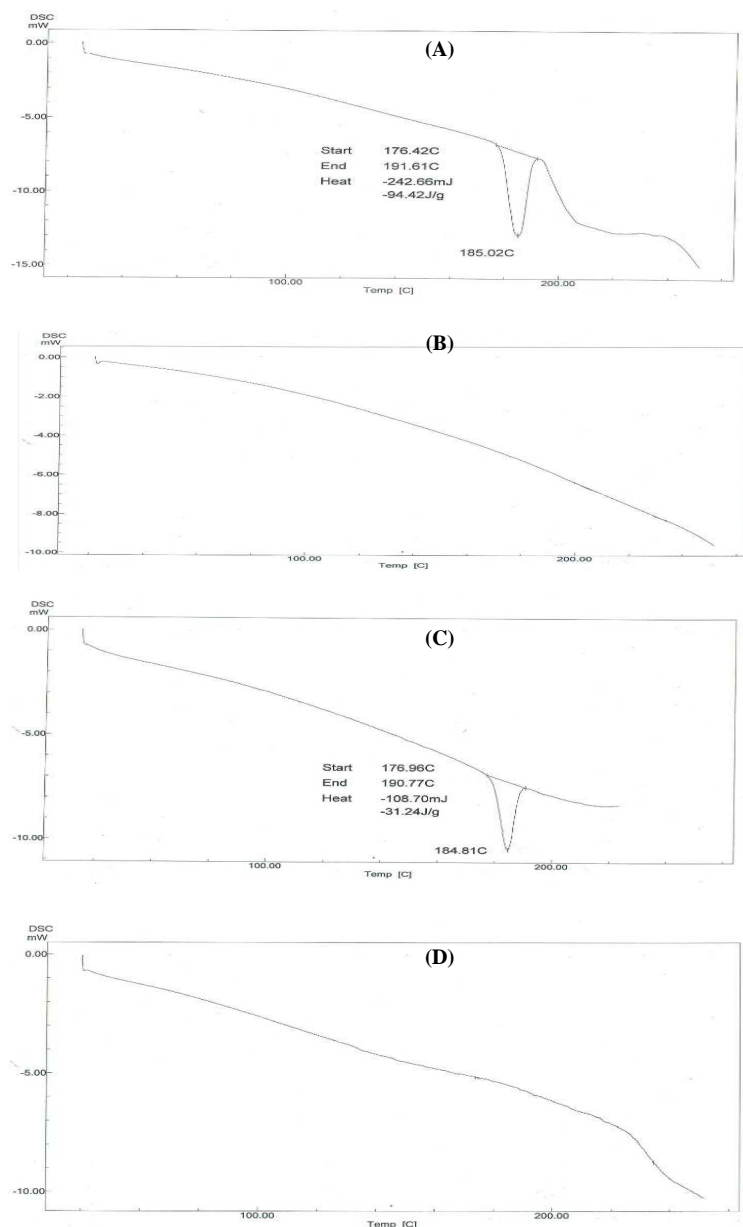


Fig. 33. DSC thermograms of (A) pure IRB (B) Aerosil 200 (C) physical mixture of IRB and Aerosil 200 (D) S-SNEDDS formula (F3)

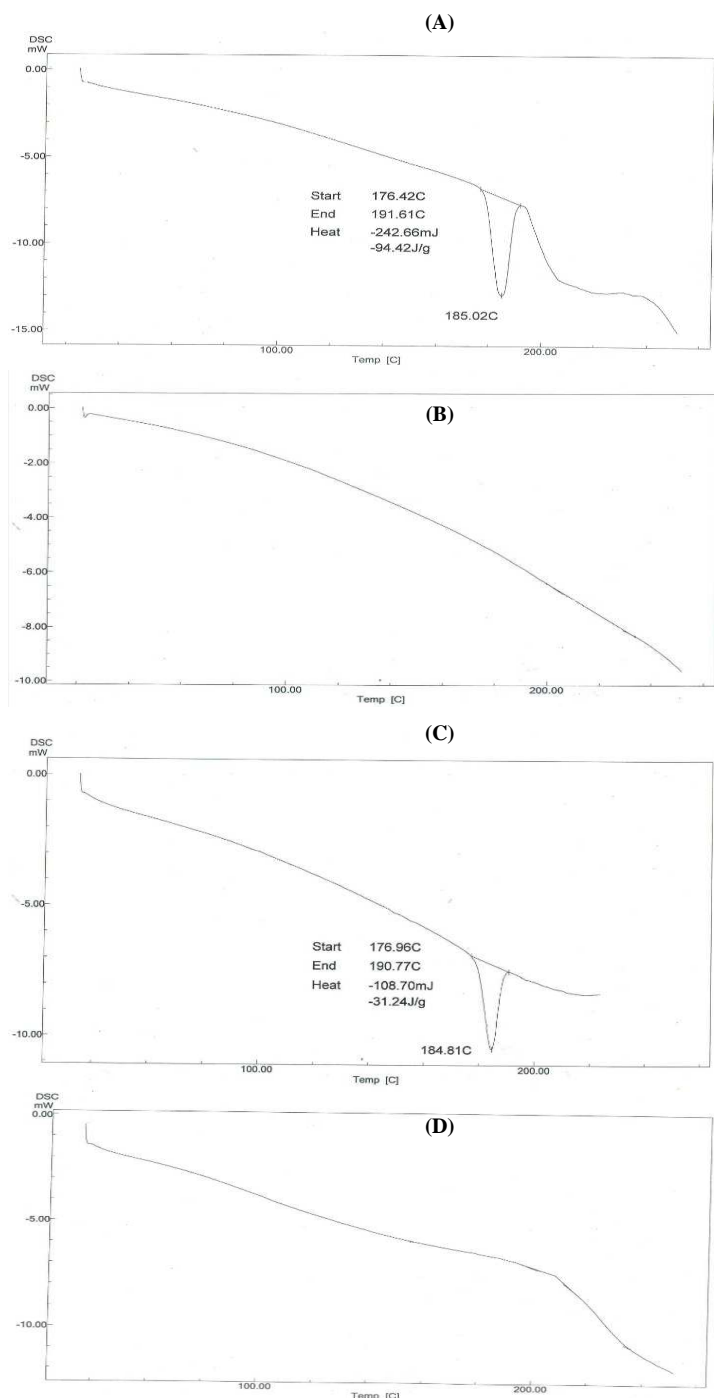


Fig. 34. DSC thermograms of (A) pure IRB (B) Aerosil 200 (C) physical mixture of IRB and Aerosil 200 (D) S-SNEDDS formula (F5)

### 3.4.5. Fourier Transformed Infrared Spectroscopy (FTIR)

FTIR spectra are mainly used to determine interaction between the drug and any of the excipients used. The presence of interaction is detected by the disappearance of important functional group of the drug. The IR spectrum of IRB showed broad band at  $3435\text{ cm}^{-1}$  for N-H group, a strong sharp peak at  $1731\text{ cm}^{-1}$  for C=O group, two peaks for aromatic C=C stretching at  $1562\text{ cm}^{-1}$  and  $1440\text{ cm}^{-1}$ , a peak for  $sp^2$  C-H stretching at  $3060\text{ cm}^{-1}$  and two peaks for  $sp^3$  C-H at  $2958\text{ cm}^{-1}$  and  $2871\text{ cm}^{-1}$ . Similar peaks were observed in the spectra of physical mixture and prepared S-SNEDDS formulae (F3 and F5), along with absence of interfering peaks indicating there is no unwanted interaction between IRB and other used excipients in the study as shown in figures (35-36).

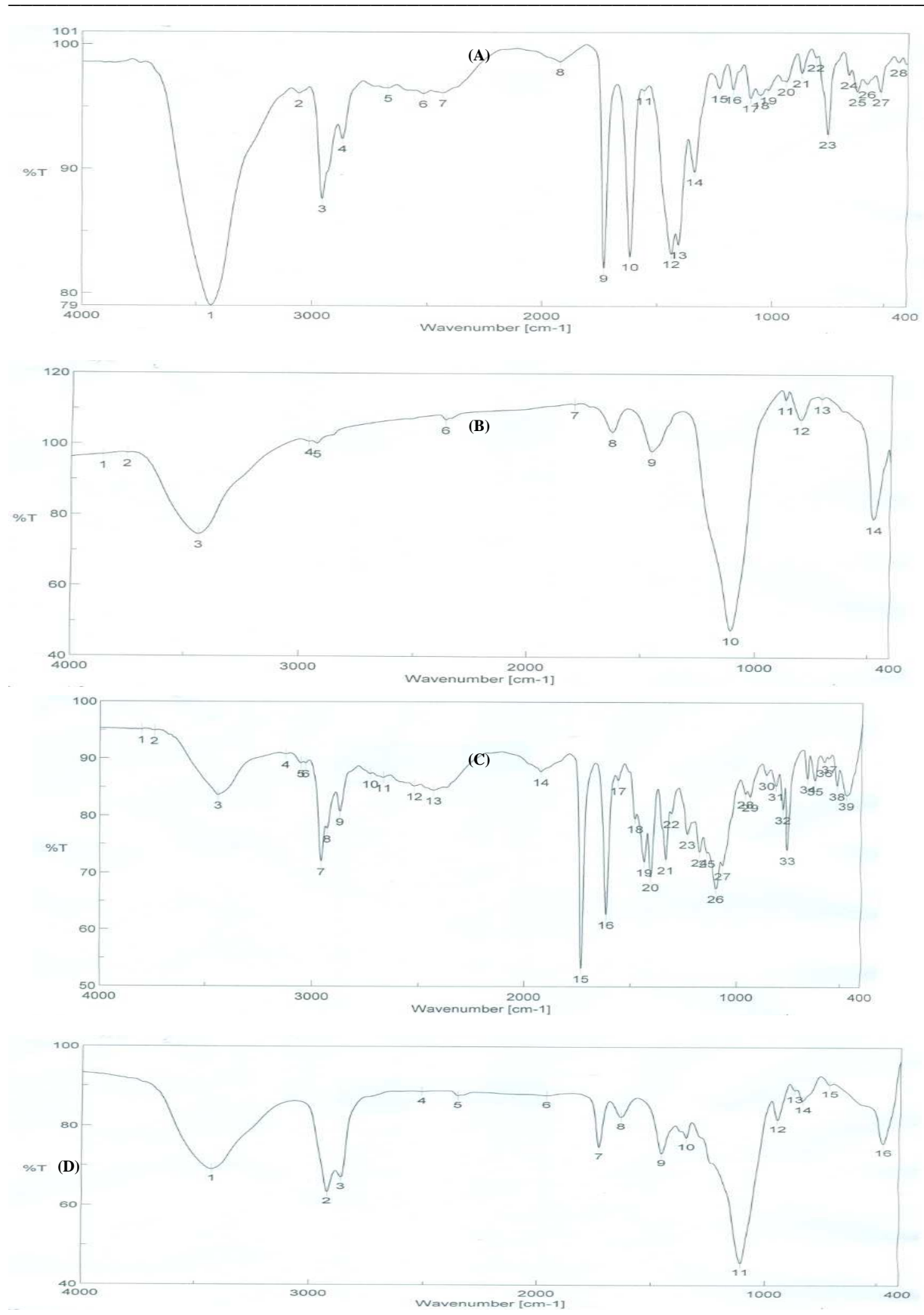


Fig. 35. FTIR spectra of (A) IRB (B) Aerosil 200 (C) Physical mixture of IRB and Aerosil 200 (D) S-SNEDDS formula (F3)

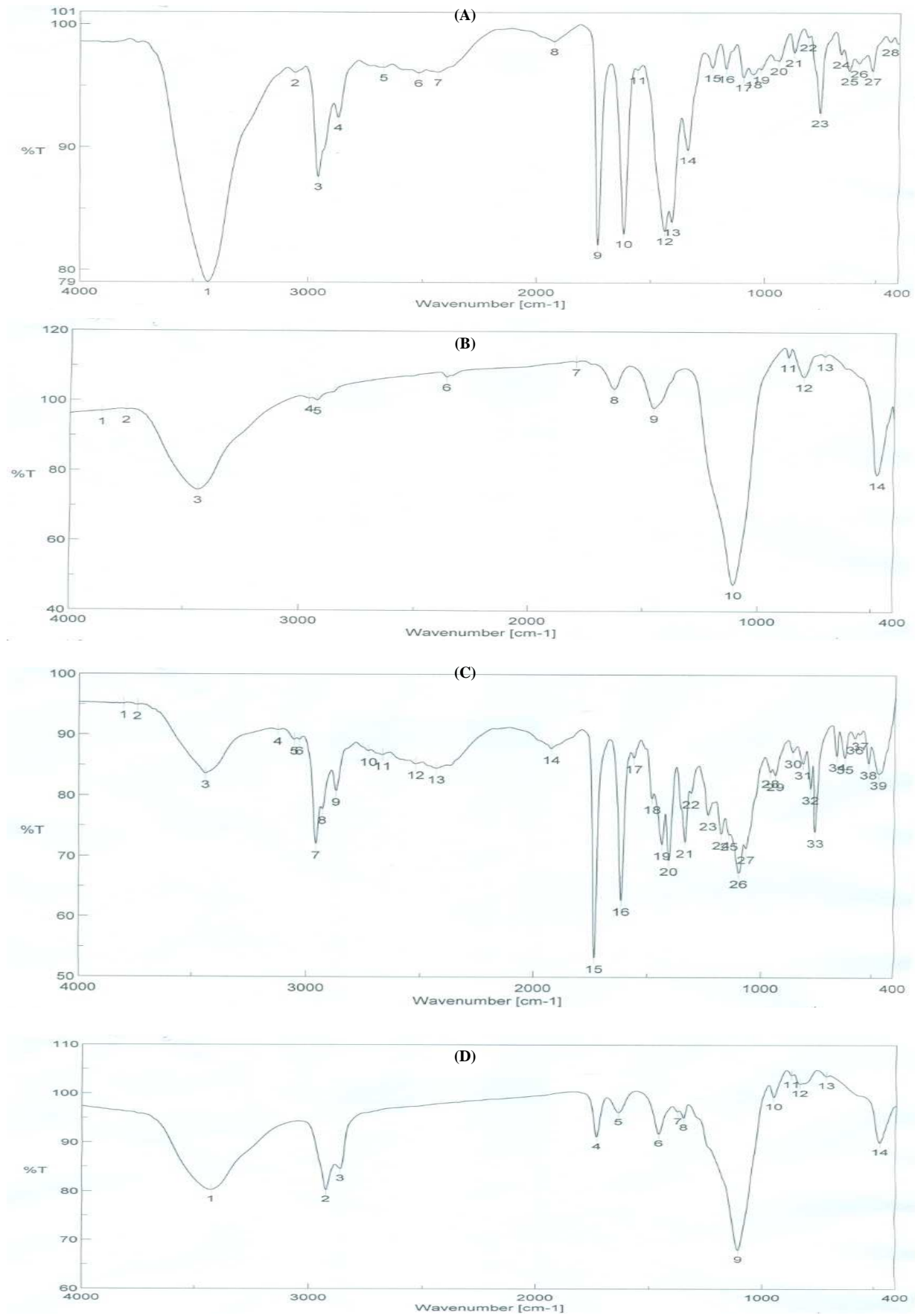


Fig. 36. FTIR spectra of (A) IRB (B) Aerosil 200 (C) Physical mixture of IRB and Aerosil 200 (D) S-SNEDDS formula (F5)

### 3.4.6. Drug loading efficiency

The amount of drug present in the two optimized S-SNEDDS formulae was found to be within USP limit. The drug loading efficiency was found to be  $96.89 \pm 1.37$  for formula F3 and  $98.60 \pm 1.45$  for formula F5. The drug content in S-SNEDDS of IRB was almost identical with the results obtained in liquid SNEDDS so there is no change of percentage drug content after conversion of liquid to solid SNEDDS using spray drying technique. These results were in a good agreement with high drug content found by Bhagwat *et al.* who prepared solid self micro emulsifying drug delivery system of telmisartan [21].

### 3.4.7. In-vitro drug release studies

The percentage drug release from S-SNEDDS was found to be higher than that of pure drug and marketed product as shown in figure (37). Cumulative % drug release of IRB from S-SNEDDS was found to be  $89.64 \pm 0.90\%$  and  $92.08 \pm 0.93\%$  for formulae F3 and F5 respectively within the initial one hour. However, within the same time period of the dissolution study, only  $9.73 \pm 0.54\%$  and  $43.34 \pm 1.49\%$  of IRB was dissolved from pure powder and marketed tablets respectively. The drug dissolution study also indicates that the self-nanoemulsifying property of the formulation remains unaffected by the conversion of the liquid SNEDDS to the solid form as illustrated in figure (38). It was also noticed that the release of IRB from S-SNEDDS was slightly lower than liquid SNEDDS. This might be attributed to the presence of adsorbent material which may delay the dissolution rate for a small extent. These findings were also compatible with Bhagwat *et al.* who found that the drug dissolution profiles of the liquid SNEDDS showed no significant differences when compared to those of the solid SNEDDS, suggesting that the SNEDDS preserves a similar performance in emulsification regardless of the form (*i.e.* liquid or solid) [21].

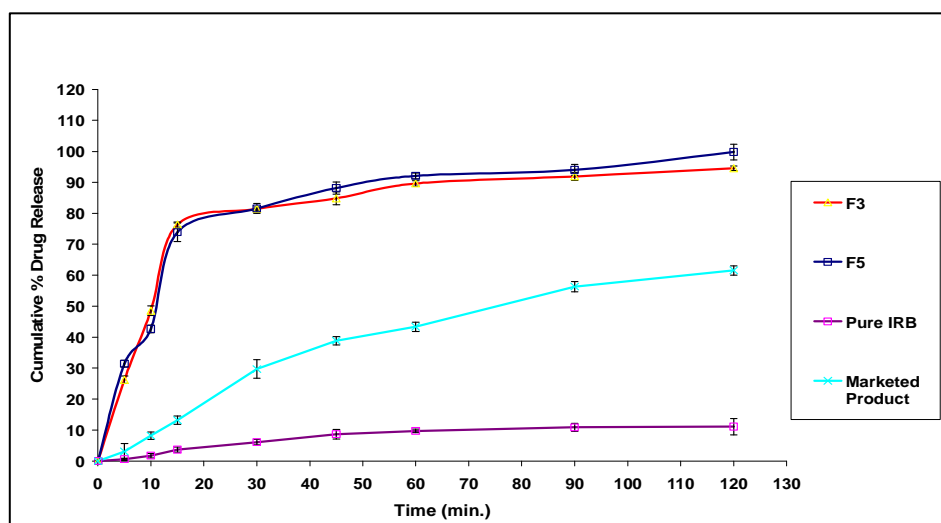


Fig. 37. *In-vitro* release profiles of IRB S-SNEDDS formulae compared with pure IRB and marketed product

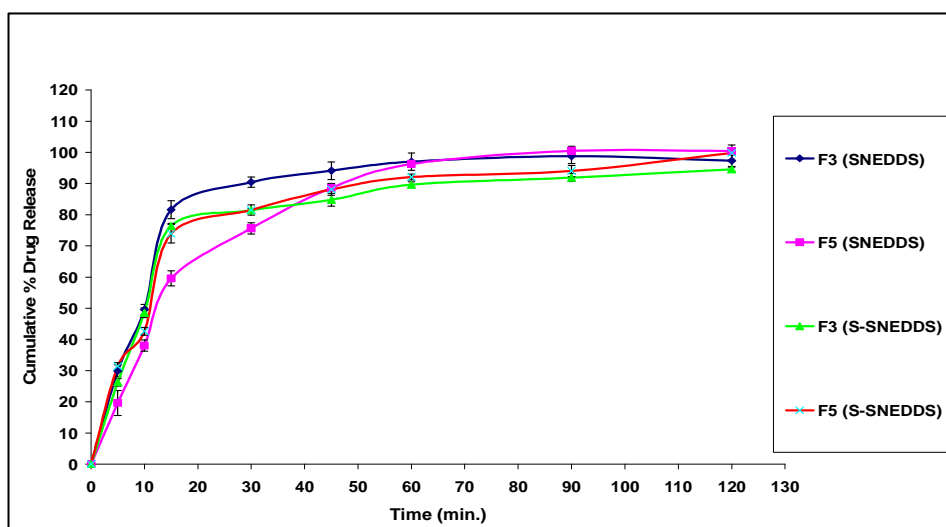


Fig. 38. Comparison study of *In-vitro* release profiles of IRB SNEDDS formulae and S-SNEDDS formulae (F3&F5)

## CONCLUSION

In this study, a novel liquid SNEDDS consisting of Capryol 90, Cremophor RH40 and Transcutol HP as an oil phase, surfactant and co-surfactant, respectively, was formulated and further developed into a solid SNEDDS by a spray-drying technique using Aerosil 200 as the solid carrier. From this study it was concluded that the prepared liquid SNEDDS was thermodynamically stable with good self emulsification efficiency and having globule size in nanometric range which may be physiologically stable. Study also concluded that S-SNEDDS of IRB prepared by a spray-drying technique using Aerosil 200 as the solid carrier have good flow properties and drug content. This solid SNEDDS preserved the self-emulsification performance of the liquid SNEDDS and gave a faster *in-vitro* dissolution rate than the crude powder and marketed product. Results of SEM demonstrate that spherical particles of S-SNEDDS can be obtained without agglomeration. Considering the limitations associated with liquid SNEDDS, a solid powder formulation should be a more acceptable form. Furthermore, our results suggest that the S-SNEDDS could be considered and further evaluated for the oral delivery of lipophilic poorly soluble drugs for which an oral route of administration is desirable. In conclusion, Self emulsifying drug delivery systems were a promising approach for the formulation of IRB. S-SNEDDS appeared to be an interesting approach to improve problems associated with oral delivery of IRB. Thus S-SNEDDS can be considered as novel and commercially feasible alternative to current marketed IRB. Finally, the oral delivery of hydrophobic drugs can be made possible by S-SNEDDS, which have been shown to substantially improve the oral bioavailability.

## Acknowledgement

Authors would like to thank MSc. Botros Yossef, assistant lecturer at organic chemistry department, Sinai University who helped us in the DSC and FTIR interpretations.

## REFERENCES

- [1] T Kommuru; B Gurley; M Khan; I Reddy, *Int. J. Pharm.*, **2001**, 212, 233–246.
- [2] R Gursoy; S Benita, *Biomed. Pharm. Ther.* **2004**; 58: 173–182.
- [3] S Nazzal; I Smalyukh; O Lavrentovich; M Khan, *Int. J. Pharm.*, **2002**, 235, 247–265.
- [4] T Iosio; D Voinovich; M Grassi; J Pinto; B Perissutti; M Zacchigna, *Eur. J. Pharm. Biopharm.*, **2008**, 69(2), 686–697.
- [5] T Yi; J Wan; H Xu; X Yang, *Eur. J. Pharm. Biopharm.*, **2008**, 70(2), 439–444.
- [6] B Tang; G Cheng; J GU; C Xu, *Drug Discov. Today*, **2008**, 13(13-14), 606–612.
- [7] Y Chen; G Li; X Wu; Z Chen; J Hang; B Qin, *Biol. Pharm. Bull.*, **2008**, 31(1), 118–125.
- [8] B Kang; J Lee; S Chon, *Int. J. Pharm.*, **2004**, 274, 65–73.
- [9] L Wang; J Dong; J Chen; J Eastoe; X Li, *J. Colloid Interface Sci.*, **2009**, 330, 443–448.
- [10] M Ishida; R Tawa; N Shibata; K Takada, *J. Control. Release*, **2005**, 105, 23–31.
- [11] K Kishanta; S Uma; P Subasini; M Debananda; P Ghanshyam; C Kanhu, *Int. J. Pharm. & Bio. Sci.*, **2011**, 2(4), 1114–1122.
- [12] J Patel; A Patel; M Raval; N Sheth, *J. Adv. Pharm. Tech. Res.*, **2011**, 2(1), 9–16.
- [13] R Dixit; M Nagarsenker, *Eur. J. Pharm. Sci.*, **2008**, 35, 92–183.
- [14] A Date; M Nagarsenker M, *Int. J. Pharm.*, **2007**, 329, 166–172.
- [15] A Patel; P Vavia, *AAPS J.*, **2007**, 9, 344–352.
- [16] B Divyakumar; B Priyanka; B Kiran, *As. J. Biomed. & Pharm. Sci.*, **2012**, 2, 7–14.
- [17] S Sheikh; F Shakeel; S Talegaonkar; F Ahmad; R Khar; M Ali, *Eur. J. Pharm. Biopharm.*, **2007**, 66, 227–243.
- [18] E Atef; A Belmonte, *Eur. J. Pharm. Sci.*, **2008**, 35, 257–263.
- [19] I Ehab; A Saleh; M Ahmed; A Mansoor, *Int. J. Pharm.*, **2004**, 285, 109–119.
- [20] K Ashok; S Kuldeep; K Murugesh; R Sriram; M Ramesh, *Acta Pharm.*, **2012**, 62, 563–580.
- [21] A Bhagwat; I D'Souza, *Int. J. Drug Develop. & Res.*, **2012**, 4(4), 398–407.
- [22] D Mahajan; T Shaikh; D Baviskar; R Wagh, *Int. J. Pharm. Pharm. Sci.*, **2011**, 3(4), 163–166.
- [23] P Balakrishnan; B Lee; D Oh; J Kim; M Hong; J Jee; J Kim; B Yoo; J Woo; C Yong; H Choi, *Int. J. Pharm.*, **2009**, 374, 66–72.
- [24] P Ghosh; R Majithiya; M Umrethia; S Murthy, *AAPS Pharm. Sci. Tech.*, **2006**, 7, 172–177.
- [25] A Naseem; T Sushama; K Roop; J Manu, *J. Biomed. Nanotechnol.*, **2013**, 9, 1–14.
- [26] Z Yi; W Changguang; H Albert; R Ke; G Tao; Z Zhirong; Z Ying, *Int. J. Pharm.*, **2010**, 383, 170–177.
- [27] B Zakia; Z Suyang; Z Wenli; W Junlin, *Int. J. Pharm.*, **2013**, 29, 1103–1113.
- [28] P Kadu; S Kushare; D Thacker; S. Gattani, *Pharm. Develop. & Tech.*, **2011**, 16(1), 65–74.
- [29] J Odeberg; P Kaufmann; K Kroon; P Hoglund, *Eur. J. Pharm. Sci.*, **2003**, 20, 375–382.
- [30] D Yi; A Jung; K Mi; K Bong; S Chul; G Han, *Biol. Pharm. Bull.*, **2011**, 34(8), 1179–1186.
- [31] C Sajeev; G Vinay; R Archana; R Saha, *J. Microencap.*, **2002**, 19, 753–760.

- [32] A Durgacharan; I John, *Int. cur. Pharm J.*, **2012**, 12, 414–419.
- [33] R Surender; R Mahalaxmi; P Srinivas; K Deepak; K Amit; P Sneha, *J. Chem. Pharm. Res.*, **2011**, 3(2), 280–289.
- [34] M Reddy; T Rehana; S Ramakrishna; K Chowdary; V Prakash, *AAPS PharmSciTech.*, **2004**, 6(1), 68–76.
- [35] J Tang, *Cur. Drug Ther.*, **2007**, 2, 85–93.
- [36] A Humberstone; W Charman, *Adv. Drug Deliv. Rev.*, **2008**, 25, 103–128.
- [37] M Chen, *Adv. Drug Deliv. Rev.*, **2008**, 60, 768–777.
- [38] P Balakrishnan; B Lee; D Oh; J Kim; M Hong; J Jee, *Eur. J. Pharm. Biopharm.* **2009**, 72, 539–545.
- [39] S Charman; W Charman; M Rogge; T Wilson; F Dutko; C Pouton, *Pharm. Res.*, **1992**, 9, 87–93.
- [40] A Azeem; M Rizwan; F Ahmad; Z Iqbal; R Khar; M Aqil; S Talegaonkar, *AAPS PharmSciTech.*, **2009**, 10, 69–76.
- [41] C O’Driscoll, *Eur. J. Pharm. Sci.*, **2002**, 15, 405–415.
- [42] G Urvasi; A Ritika; A Geeta, *Acta Pharm.*, **2012**, 62, 357–370.
- [43] Y Elnaggar; M El-Massik; Y Abdallah, *Int. J. Pharm.*, **2009**, 380, 133–141.
- [44] S Anuradha; A Pratikkumar; H Darshana, *Int. J. Pharm. Biosci. Technol.*, **2013**, 1, 89–101.
- [45] R Farinato; R Rowell, *Encyclopedia of emulsion technology*, Marcel Dekker, New York, **2000**, 1, 439–479.
- [46] M Lawrence, *Curr. Colloid Interface Sci.*, **1996**, 1, 826–832.
- [47] C Pouton, *Eur. J. Pharm. Sci.*, **2000**, 11, 93–98.
- [48] A Spornath; A Yagmur; A Aserin; R Hoffman; N Garti, *J. Agri. Food Chem.*, **2002**, 50, 6917–6922.
- [49] P Lia; A Ghosh; R Wagner; S Krill; Y Joshi, *Int. J. Pharm.*, **2005**, 288, 27–34.
- [50] V Kallakunta; S Bandari; R Jukanti; P Veerareddy, *Powder Technol.*, **2012**, 221, 375–382.
- [51] B Sharma; S Sharma; S Gupta; M Bishnoi, *Acta Pharm.*, **2007**, 57, 315–323.
- [52] X Wu; J Xu; X Huang; C Wen, *Drug Dev. Ind. Pharm.*, **2011**, 37, 15–23.
- [53] P Nepal; H Han; H Choi, *Eur. J. Pharm. Sci.*, **2010**, 39, 224–232.
- [54] S Singh; P Verma, *Arch. Pharm. Res.*, **2009**, 32, 1629–1635.
- [55] S Nazzal; M Nutan; A Palamakula; R Shah; A Zaghoul; M Khan, *Int. J. Pharm.*, **2002**, 240, 103–114.
- [56] J Hong; J Kim; Y Song; J Park; C Kim, *J. Control. Release*, **2006**, 110, 332–338.
- [57] S Rai; M Yasir, *IOSR J. Pharm.*, **2012**, 2, 47–56.
- [58] J Maulik; M Natvarlal; B Ritesh; P Rakesh, *As. J. Pharm. Sci.*, **2010**, 5, 266–275.
- [59] D Ashish; N Premchand; Y Pramod, *Der Pharmacia Lettre*, **2010**, 2(2), 94–106.
- [60] K Margulis; S Magdassi, *Nanomed.*, **2009**, 5, 274–281.
- [61] C Pouton; S Porter, *Adv. Drug Deliv. Rev.*, **2008**, 60, 625–637.
- [62] Ghai; V Sinha, *Nanomed.*, **2011**, 8(5), 618–626.
- [63] C Chun; H Linna, *J. App. Pharm. Sci.*, **2011**, 1(10), 195–199.